Theoretical studies of high-power laser ionization of molecules in the tunneling region

K. Mishima,[1] K. Nagaya,[1] M. Hayashi,[2] and S. H. Lin[1]
[1]*Institute of Atomic and Molecular Sciences, Academia Sinica, P. O. Box 23-166, Taipei 10764, Taiwan, Republic of China*
[2]*Center for Condensed Matter Sciences, National Taiwan University, Taipei 106, Taiwan, Republic of China*
(Received 14 July 2004; published 29 December 2004)

In this paper, we extend our previous works on the generalization of Keldysh's theory to the photoionization processes of molecules. In particular, we include the Franck-Condon factors into our photoionization rate formulas which are based on the use of the molecular orbital theory to describe the electronic degrees of freedom. The inclusion of Franck-Condon factors leads to the proper treatment of the molecular vibrational degrees of freedom. All of our formulas consist of the preexponential and exponential factors, and have explicit laser frequency dependence in the same manner as the original atomic Keldysh theory. The latter fact facilitates the exploration of the laser frequency dependence of the photoionization rate, which is more advantageous than the popular Ammosov-Delone-Krainov formulas. As a result, our analytical expressions turn out to be quite instructive to deduce physical meanings of the photoionization processes of molecules. As an illustrative example, we have applied our formulas to the photoionization process of H_2 molecules and found that our formulas reproduce the numerical results reported in the literature quite well. Without the Franck-Condon factors, our formulas cannot fit the numerical results well, which implies the importance of including properly the Franck-Condon factors for the tunneling photoionization processes of molecules. The results also indicate that the exponential factors which depend on the nuclear equilibrium state play a key role in determining the photoionization rates of the spatially aligned molecules. Comparing the Condon and non-Condon approximations shows that the Condon approximation is usually appropriate for the case of the laser polarization perpendicular to the molecular axis, while it is not necessarily true for the parallel case. Our theoretical results are also applied to analyze the experimental data of Urbain *et al.* [Phys. Rev. Lett. **92**, 163004 (2004)] for the photoionization process of H_2 molecules.

DOI: 10.1103/PhysRevA.70.063414 PACS number(s): 32.80.Rm, 33.80.Rv, 32.80.Fb

I. INTRODUCTION

In recent years, many theoretical and experimental studies on the interaction between the laser field and the matters have been directed to the detailed investigation on molecular photoionization processes in intense laser fields. Different from the photoionization processes of atoms, due to multinuclei in nature, molecules exhibit interesting features which cannot be adequately explained by the atomic theories.

For atomic tunneling photoionization, Keldysh-Faisal-Reiss (KFR) [1–3] and Ammosov-Delone-Krainov (ADK) [4] theories are frequently utilized for the analyses of the experimental data. In general, these theories can reproduce the experimental results of the atomic photoionization very well. However, in recent years, the *atomic* ADK model has found more widespread use [4]. One of the reasons for this may be due to the fact that the ADK theory succeeds in predicting or reproducing experimental results much better than the KFR theory. In addition, the formalism of the ADK model is much simpler. Although it is an atomic theory, ADK theory has been applied to simple molecular systems like H_2, O_2, N_2, etc. However, it should be recognized that the ADK theory is the *atomic* theory, *not the molecular* one and can be applied to tunneling ionization and not to photoionization

For molecular systems, in addition to multielectrons contributed from multinuclei, the molecular motion like rotation, vibration, etc. has to be taken into account properly. However, this has been neglected in some theoretical studies [5,6]. The importance of the nuclear degrees of freedom has been reported in several works from the theoretical [7–9] and experimental [10] points of view. The neglect of molecule-specific degrees of freedom may cause serious problems especially if one is working with large polyatomic molecules. This has already been pointed out by Saenz [8].

Recently, molecular ADK theory has been proposed by Lin and co-workers [6], and the so-called intense-field many-body *S*-matrix theory (IMST) has been developed for atoms and later extended for the molecular systems by Faisal and co-workers [11]. These theories appear to be able to reproduce experimental results quite well. As an alternative, many numerical calculations have been carried out for simple molecules by a number of research groups [12], but because of the huge computational efforts involved even for diatomic molecules, these approaches are not promising for larger molecules at present.

In our previous papers [13], we have generalized the Keldysh theory [1], which was originally developed for the ionization of the 1*s* state of hydrogenlike atoms. We have treated the ionization of molecules by introducing the molecular orbital theory within the one-center approximation and calculated the photoionization rates of molecules by extending the Coulomb-Volkov function of atomic systems to the molecular counterpart and expressing the initial molecular state by a linear combination of atomic orbitals and molecular orbitals (LCAO MO).

In the present work, we shall extend our previous formulations of the photoionization of molecules by introducing the Born-Oppenheimer approximation to properly take into consideration the electronic and nuclear degrees of freedom. For the electronic part, we use the molecular orbital theory; in particular, we use the LCAO MO theory for the initial

 ©2004 The American Physical Society

electronic orbital state and the Volkov function for the final electronic state of photoionized electron. In treating the nuclear part of photoionization of molecules, the Condon effect and the non-Condon effect arise. This formulation can treat the photoionization of not only diatomic molecules, but also polyatomic molecules, and as application and illustration, it will be applied to calculate the photoionization rate of H_2. Our computed results will be compared with experimental data.

The present paper is organized as follows. In Sec. II, we derive the theoretical aspects of our method mentioned above in detail. In Sec. III, the details of the *ab initio* calculation of H_2, the calculation of potential energy curves (PECs) of H_2^+ deformed by the laser field, and the calculation of Franck-Condon factors are described. In Sec. IV, we demonstrate our numerical photoionization rates of H_2 using the formula derived in Sec. V. We investigate two cases where the laser polarization direction is parallel and perpendicular to the molecular axis. The behaviors of the two cases are quite different, which agrees with the previously reported work [14]. In addition, we compare Condon and non-Condon approximations. This comparison shows that the more accurate molecular photoionization rate can be obtained by taking into account the relative geometries between the neutral and ionic potential energy surfaces and the characteristics of the ionic potential itself in addition to the equilibrium neutral state. The concluding remarks are given in Sec. V.

II. THEORY

A purpose of this section is to derive the photoionization rate of molecules within the approximation of the atomic Keldysh theory. According to the time-dependent perturbation theory, we have

$$i\hbar\frac{\partial\Psi}{\partial t}=\hat{H}\Psi, \tag{2.1}$$

where

$$\hat{H}=\hat{H}_0+\hat{H}' \tag{2.2}$$

and

$$i\hbar\frac{\partial}{\partial t}\Psi_n^0(q,t)=\hat{H}_0\Psi_n^0(q,t), \tag{2.3}$$

where $\hat{H}_0$ is the zero-order Hamiltonian and $\hat{H}'$ the perturbation. If the system is initially in the kth state, then from

$$\Psi(q,t)=\sum_n c_n(t)\Psi_n^0(q,t) \tag{2.4}$$

we obtain

$$i\hbar\frac{dc_m(t)}{dt}=\langle\Psi_m^0(q,t)|\hat{H}'|\Psi_k^0(q,t)\rangle. \tag{2.5}$$

In the dipole approximation, $\hat{H}'$ is given by

$$\hat{H}'=-\mathbf{M}\cdot\mathbf{F}(t), \tag{2.6}$$

where

$$\mathbf{M}=-e\sum_{i=1}^{N_e}\mathbf{r}_i \tag{2.7}$$

is the dipole operator. Here, N_e represents the number of the electrons in the system, $\mathbf{r}_i$ the position of the ith electron, and

$$\mathbf{F}(t)=\mathbf{F}\cos\omega t, \tag{2.8}$$

the optical electric field.

For molecular systems, the Born-Oppenheimer approximation is commonly used; thus for the photoionization from the initial rovibronic state av to the ionized rovibronic state pv', we find

$$i\hbar\frac{dc_{pv'}(t)}{dt}=\langle\Psi_{pv'}^0(q,t)|\hat{H}'|\Psi_{av}^0(q,t)\rangle, \tag{2.9}$$

where a and p denote the initial bound electronic state and the final ionized electronic state, respectively, while v and v' represent their corresponding rovibrational states. For example, for the case of diatomic molecules, if the molecular ion is a stable species, then we have the Franck-Condon transition between the discrete rovibrational states.

If we let $\Theta_{pv'}$ and Θ_{av} represent the rovibrational wave functions with energies $E_{pv'}$ and E_{av}, then Eq. (2.9) can be written as

$$i\hbar\frac{dc_{pv'}(t)}{dt}=\langle\Theta_{pv'}|H'_{pa}(t)|\Theta_{av}\rangle\exp\left\{\frac{it}{\hbar}(E_{pv'}-E_{av})\right\}, \tag{2.10}$$

where $H'_{pa}(t)$ denotes the electronic matrix element of the dipole interaction. If the molecule is initially in a closed-shell bound state a, then for the case of one-electron ionization, $H'_{pa}(t)$ can be written as

$$H'_{pa}(t)=-\sqrt{2}\langle\phi_{\mathbf{p}}|\boldsymbol{\mu}\cdot\mathbf{F}(t)|\phi_a\rangle, \tag{2.11}$$

where ϕ_a denotes the highest occupied molecular orbital (HOMO) while $\phi_{\mathbf{p}}$ represents the ionized electronic wave function. For the Keldysh theory, $\phi_{\mathbf{p}}$ is described by the Volkov function, i.e., the plane-wave state of the emitted electron dressed by the laser field defined in the length gauge:

$$\phi_{\mathbf{p}}(\mathbf{r},t)=\exp\left[\frac{i}{\hbar}\left\{[\mathbf{p}-e\mathbf{A}(t)]\cdot\mathbf{r}-\frac{1}{2m}\int_0^t dt'[\mathbf{p}-e\mathbf{A}(t')]^2\right\}\right]. \tag{2.12}$$

In the present work, we shall concentrate on the derivation and calculation of the following process:

$$H_2\rightarrow H_2^+ + e^-. \tag{2.13}$$

In this case, $\phi_a=\phi_{\sigma 1s}$ and using the LCAO MO theory,

$$\phi_{\sigma 1s}=b_1\chi_{1,1s}+b_2\chi_{2,1s}, \tag{2.14}$$

where $\chi_{1,1s}$ and $\chi_{2,1s}$ represent the $1s$ orbitals of nuclei 1 and 2, respectively, and b_1 and b_2 are the molecular orbital coefficients for nuclei 1 and 2, respectively. If the laser in-

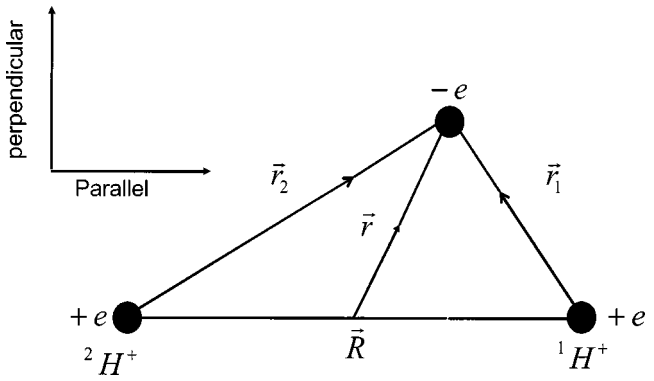

FIG. 1. Configuration of the hydrogen molecular ion H_2^+ composed of two hydrogen nuclei $^1H^+$ and $^2H^+$, and one electron e^-. The vector **R** denotes the internuclear distance directing from $^2H^+$ to $^1H^+$, **r** the position of the electron from the center of mass of the molecule, and $\mathbf{r}_1$ and $\mathbf{r}_2$ the positions of the electron measured from $^1H^+$ and $^2H^+$, respectively. On the left-hand side, the polarization direction of the linearly polarized electric field is indicated by the arrows.

tensity is not so strong or the molecular axis is perpendicular to the direction of the laser polarization, we can simply write

$$\phi_{\sigma 1s} = \frac{\chi_{1,1s} + \chi_{2,1s}}{\sqrt{2 + 2S_{12}}}, \tag{2.15}$$

where S_{12} denotes the overlap integral. It should be noted that a better basis set than the simple LCAO MO theory can be used. For polyatomic molecules, ϕ_a will be much more complicated than that used in Eq. (2.14).

Using Eq. (2.12), we obtain

$$\begin{aligned} H'_{pa}(t) &= -\sqrt{2}\sum_{j=1}^{2} b_{j,1s}\langle \phi_{\mathbf{p}}(\mathbf{r},t)|\boldsymbol{\mu}_j(\mathbf{r})\cdot\mathbf{F}(t)|\chi_{j,1s}(\mathbf{r}_j)\rangle \\ &= -\sqrt{2}\sum_{j=1}^{2} b_{j,1s}\langle \phi_{\mathbf{p}}(\mathbf{r}_j,t)|\boldsymbol{\mu}_j(\mathbf{r}_j)\cdot\mathbf{F}(t)|\chi_{j,1s}(\mathbf{r}_j)\rangle \\ &\quad\times\exp\left\{-\frac{i}{\hbar}[\mathbf{p}-e\mathbf{A}(t)]\cdot\mathbf{R}_j\right\}, \end{aligned} \tag{2.16}$$

where we have defined

$$\mathbf{R}_1 = \frac{\mathbf{R}_{0a}}{2} \quad \text{and} \quad \mathbf{R}_2 = -\frac{\mathbf{R}_{0a}}{2}. \tag{2.17}$$

The vector $\mathbf{R}_{0a}$ is the instantaneous internuclear vector of H_2. In deriving this equation, we have used the notation defined in Fig. 1.

In the Keldysh notation, we have

$$\begin{aligned} V_{0,1s}[\mathbf{p}-e\mathbf{A}(t)] &= \langle \phi_{\mathbf{p}}(\mathbf{r}_j,t)|\boldsymbol{\mu}_j(\mathbf{r}_j)\cdot\mathbf{F}|\chi_{j,1s}(\mathbf{r}_j)\rangle \\ &\quad\times\exp\left\{-\frac{i}{2m\hbar}\int_0^t dt[\mathbf{p}-e\mathbf{A}(t')]^2\right\}. \end{aligned} \tag{2.18}$$

In the above equations, we have defined the vector potential $\mathbf{A}(t)$ associated with the laser pulse $\mathbf{F}(t)$ as follows:

$$\mathbf{A}(t) = -\frac{\mathbf{F}}{\omega}\sin\omega t. \tag{2.19}$$

Therefore, we obtain

$$\begin{aligned} H'_{pa}(t) &= -\sqrt{2}\sum_{j=1}^{2} b_{j,1s}V_{0,1s}[\mathbf{p}-e\mathbf{A}(t)]\cos\omega t \\ &\quad\times\exp\left[\frac{i}{\hbar}\left\{\frac{1}{2m}\int_0^t dt'[\mathbf{p}-e\mathbf{A}(t')]^2\right.\right. \\ &\quad\left.\left.-[\mathbf{p}-e\mathbf{A}(t)]\cdot\mathbf{R}_j\right\}\right]. \end{aligned} \tag{2.20}$$

For the photoionization process of H_2, if $H'_{pa}(t)$ does not change significantly with vibration, we can use the so-called Condon approximation in Eq. (2.10) to obtain

$$\begin{aligned} &i\hbar\frac{dc_{pv'}(t)}{dt} \\ &= -\sqrt{2}\langle\Theta_{pv'}|\Theta_{av}\rangle\sum_{j=1}^{2} b_{j,1s}V_{0,1s}[\mathbf{p}-e\mathbf{A}(t)]\cos\omega t \\ &\quad\times\exp\left[\frac{i}{\hbar}\left\{(E_{pv'}-E_{av})t+\frac{1}{2m}\int_0^t dt'[\mathbf{p}-e\mathbf{A}(t')]^2\right.\right. \\ &\quad\left.\left.-[\mathbf{p}-e\mathbf{A}(t)]\cdot\mathbf{R}_j\right\}\right]. \end{aligned} \tag{2.21}$$

Finally, the photoionization rate can be written as

$$\begin{aligned} w_{av\to pv'} &= 2\lim_{T\to\infty}\int\frac{d^3p}{(2\pi\hbar)^3}\mathrm{Re}[\dot{c}^*_{pv'}(T)c_{pv'}(T)] \\ &= \frac{4}{\hbar^2}\lim_{T\to\infty}\mathrm{Re}\int\frac{d^3p}{(2\pi\hbar)^3}|\langle\Theta_{pv'}|\Theta_{av}\rangle|^2\sum_{j=1}^{2}\sum_{j'=1}^{2} b^*_{j,1s}b_{j',1s} \\ &\quad\times\int_0^T dt\cos\omega T\cos\omega t V^*_{0,1s}[\mathbf{p}-e\mathbf{A}(T)] \\ &\quad\times V_{0,1s}[\mathbf{p}-e\mathbf{A}(t)]\exp\left[\frac{i}{\hbar}\left\{\int_T^t dt'\left(I_{av,pv'}\right.\right.\right. \\ &\quad\left.\left.+\frac{1}{2m}[\mathbf{p}-e\mathbf{A}(t')]^2\right)+[\mathbf{p}-e\mathbf{A}(T)]\cdot\mathbf{R}_j\right. \\ &\quad\left.\left.-[\mathbf{p}-e\mathbf{A}(t)]\cdot\mathbf{R}_{j'}\right\}\right], \end{aligned} \tag{2.22}$$

where $|\langle\Theta_{pv'}|\Theta_{av}\rangle|^2$ is the Franck-Condon factor, and we define

$$I_{av,pv'} = E_{pv'} - E_{av}, \tag{2.23}$$

and the transition dipole matrix element between the plane wave and 1*s* atomic orbital is given by

$$V_{0,1s}(\mathbf{p}) = \langle \exp(i\mathbf{p}\cdot\mathbf{r}/\hbar)|e\mathbf{F}\cdot\mathbf{r}|\chi_{1s}(\mathbf{r})\rangle = -\frac{2^{13/4}\sqrt{\pi}ieFp_z\hbar^{5/2}I_{1s}^{5/4}}{m^{7/4}(I_{1s}+p^2/2m)^3}. \quad (2.24)$$

Performing the integration over t and taking the limit $T\to\infty$ render

$$w_{av\to pv'} = \frac{4\pi}{\hbar}\mathrm{Re}\sum_{j=1}^{2}\sum_{j'=1}^{2} b_{j,1s}^{*}b_{j',1s}\int\frac{d^3p}{(2\pi\hbar)^3} \times \sum_{n=-\infty}^{\infty} L_{j,1s}^{*}(\mathbf{p})L_{j',1s}(\mathbf{p})\,\delta\left(I_{av,pv'}+\frac{p^2}{2m}+\frac{e^2F^2}{4m\omega^2}-n\hbar\omega\right), \quad (2.25)$$

where

$$L_{j,1s}(\mathbf{p}) = \frac{1}{2\pi}\oint du V_{0,1s}\left(\mathbf{p}+\frac{e\mathbf{F}}{\omega}u\right) I_C\left(-\frac{1}{\hbar}\left(\mathbf{p}+\frac{e\mathbf{F}}{\omega}u\right),\mathbf{R}_j,v,v'\right)\exp\left[\frac{i}{\hbar\omega}\int_0^u\left\{I_{av,pv'}+\frac{1}{2m}\left(\mathbf{p}+\frac{e\mathbf{F}}{\omega}u'\right)^2\right\}\frac{du'}{\sqrt{1-u'^2}}\right]. \quad (2.26)$$

Here, we have defined

$$I_C(\mathbf{k},\mathbf{R}_j,v,v') = \exp(i\mathbf{k}\cdot\mathbf{R}_j)\langle\Theta_{pv'}|\Theta_{av}\rangle, \quad (2.27)$$

where the subscript C denotes the Condon approximation.

Carrying out the contour integration in the above equation and substituting it into Eq. (2.25), we obtain the general expression for the total photoionization rate of H_2 molecule from state av to pv' under the Condon approximation, which consists of the individual rates and those from the quantum interference effect [5,15,16]. The individual photoionization rate can be expressed as

$$w_{av\to pv',C}^{j,1s,j,1s} = \frac{E_{1s}|b_{j,1s}|^2|D_{j,1s,C}(I_{av,pv'})|^2|\langle\Theta_{pv'}|\Theta_{av}\rangle|^2\exp\{-2g_{j,1s,C}^{(1)}(I_{av,pv'},\mathbf{R}_j)\}}{B_{j,1s,C}(I_{av,pv'},\mathbf{R}_j)} \quad (2.28)$$

for the individual atoms $j=1$ or $j=2$, where the definitions of the terms here are

$$B_{j,1s,C}(I_{av,pv'},\mathbf{R}_j) = \left(\sinh^{-1}\gamma_{1s}+\frac{I_{av,pv'}-I_{1s}}{2I_{1s}}\frac{\gamma_{1s}}{\sqrt{1+\gamma_{1s}^2}}-\frac{\gamma_{1s}e\mathbf{F}\cdot\mathbf{R}_j}{2I_{1s}}\right)\left\{\sinh^{-1}\gamma_{1s}-\frac{\gamma_{1s}}{\sqrt{1+\gamma_{1s}^2}}+\frac{I_{av,pv'}-I_{1s}}{2I_{1s}}\frac{\gamma_{1s}^3}{(1+\gamma_{1s}^2)^{3/2}}\right\}^{1/2}, \quad (2.29)$$

$$D_{j,1s,C}(I_{av,pv'}) = \frac{1}{I_{1s}\gamma_{1s}}\left(\frac{I_{av,pv'}-I_{1s}}{\sqrt{1+\gamma_{1s}^2}}-e\mathbf{F}\cdot\mathbf{R}_j\right) - \left\{\frac{1}{\gamma_{1s}\sqrt{1+\gamma_{1s}^2}}+\frac{I_{av,pv'}-I_{1s}}{2I_{1s}}\frac{\gamma_{1s}}{(1+\gamma_{1s}^2)^{3/2}}\right\} - \frac{1}{2\hbar\omega I_{1s}}\left(\frac{I_{av,pv'}-I_{1s}}{\sqrt{1+\gamma_{1s}^2}}-e\mathbf{F}\cdot\mathbf{R}_j\right)^2, \quad (2.30)$$

$$E_{1s} = 2\sqrt{2\pi}\gamma_{1s}^4\sqrt{\frac{\omega I_{1s}}{\hbar}}, \quad (2.31)$$

$$g_{j,1s,C}^{(1)}(I_{av,pv'},\mathbf{R}_j) = \frac{1}{\hbar\omega}\left(\tilde{I}_{av,pv'}\sinh^{-1}\gamma_{1s}-\tilde{I}_{1s}\frac{\gamma_{1s}\sqrt{1+\gamma_{1s}^2}}{1+2\gamma_{1s}^2}-e\mathbf{F}\cdot\mathbf{R}_j\gamma_{1s}\right), \quad (2.32)$$

$$\tilde{I}_{av,pv'} = I_{av,pv'}+\frac{e^2F^2}{4m\omega^2}$$

(effective ionization potential of the molecule), (2.33)

$$\tilde{I}_{1s} = I_{1s}+\frac{e^2F^2}{4m\omega^2}$$

(effective ionization potential of the atomic 1s orbital), (2.34)

and

$$\gamma_{1s} = \frac{\omega\sqrt{2mI_{1s}}}{eF}$$

(Keldysh parameter of the atomic 1s orbital). (2.35)

Equation (2.28) is general in that it can be applied to any fixed molecular geometries with respect to the laser polarization direction. From Eq. (2.28), we notice that the individual

photoionization rates depend on the molecular geometry with respect to the laser polarization, which is different from atoms. They depend on the angle between the laser polarization direction and the vector of the molecular axis (due to the terms $\mathbf{F}\cdot\mathbf{R}_j$).

The quantum interference term for the transition av to pv' under the Condon approximation $w^{j,1s,j',1s}_{av\to pv',C}$ $(j\neq j')$ is given in Appendix A. It should be noted that the individual photoionization rate and the quantum interference term depend on the molecular geometry in a different way. Different from the individual ones, the quantum interference terms depend not only on the angle between the laser polarization direction and the vector of the molecular axis by the relation $\mathbf{F}\cdot\mathbf{R}_j$ but also by the angle between the molecular axis and the direction of the emitted electron [due to the term $(\mathbf{R}_j-\mathbf{R}_{j'})\cdot\hat{\mathbf{p}}$ in Eq. (A9)]. Since we integrate over the solid angle $\Omega_{\mathbf{p}}$ to obtain the total photoionization rate, the relation between the quantum interference term and the molecular geometry is not so obvious. However, we can predict that when the different nuclei lie very far from each other, the term $(\mathbf{R}_j-\mathbf{R}_{j'})\cdot\hat{\mathbf{p}}$ in Eq. (A9) will contribute to a significant extent. Therefore, the quantum interference terms are expected to be very different for small and large internuclear separations if other parameters are identical. In addition, it is likely that the angular dependence of the photoemitted electron in the quantum interference terms will be quite sensitive to the angle between the molecular axis and the direction of emitted electron in the case of a large separation of the nuclei.

Mathematically speaking, $w^{j,1s,j,1s}_{av\to pv',C}$ and $w^{j,1s,j',1s}_{av\to pv',C}$ $(j\neq j')$ are quite different. The former can always be obtained in a closed form (no numerical integration is needed) as is the case for the original atomic Keldysh theory, while in general the latter contains the numerical integration over the solid angle of the emitted electron and thus for simple molecules, $w^{j,1s,j',1s}_{av\to pv',C}$ $(j\neq j')$ can sometimes be obtained in a closed form.

In summary, the total photoionization rate of the transition $av\to pv'$ under the Condon approximation, $w_{av\to pv',C}$, is given by

$$w_{av\to pv',C}=\sum_{j=1}^{2} w^{j,1s,j,1s}_{av\to pv',C}+\sum_{j=1}^{2}\sum_{j'=1\ (j\neq j')}^{2} w^{j,1s,j',1s}_{av\to pv',C}. \tag{2.36}$$

Using the individual ionization rates and the quantum interference terms, the total photoionization rate from the initial state av under the Condon approximation is given by

$$w_{a\ v,C}=\sum_{v'} w_{av\to pv',C}. \tag{2.37}$$

Next, we derive the photoionization formulas in the tunneling limit. These can be obtained by taking the limit $\omega\to 0$ in the equations shown above. Thus, Eq. (2.28) reduces to

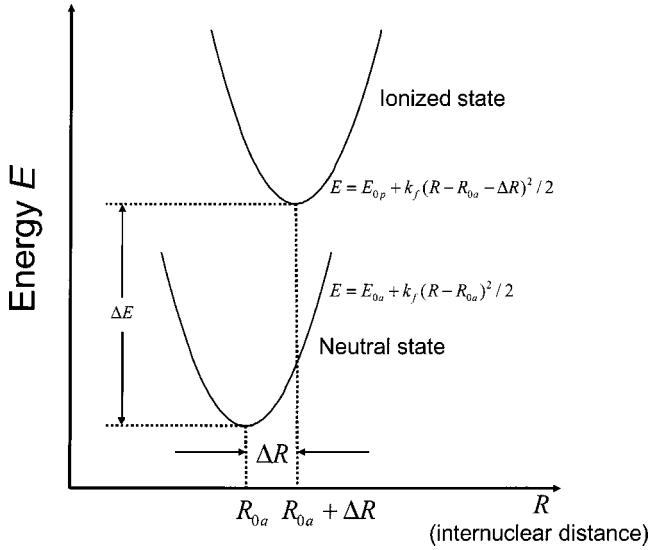

FIG. 2. Pictorial representation of the harmonic oscillator model system used for the comparison between the Condon and non-Condon approximations. The neutral and ionic PECs are identical except that the latter is displaced from the former by distance ΔR, and the energy minimum of the latter is larger than that of the former by ΔE.

$$w^{j,1s,j,1s}_{av\to pv',C,\mathrm{Tun}}=\frac{E'_{1s}|b_{j,1s}|^2|D'_{j,1s,C}(I_{av,pv'})|^2|\langle\Theta_{pv'}|\Theta_{av}\rangle|^2}{B'_{j,1s,C}(I_{av,pv'})}\times\exp\{-2h_{j,1s,C}(I_{av,pv'})\}. \tag{2.38}$$

The definitions of the terms in Eq. (2.38) are given by

$$B'_{j,1s,C}(I_{av,pv'})=\frac{I_{av,pv'}+I_{1s}-e\mathbf{F}\cdot\mathbf{R}_j}{I_{1s}}\left(\frac{3I_{av,pv'}}{I_{1s}}-1\right)^{1/2}, \tag{2.39}$$

$$D'_{j,1s,C}(I_{av,pv'})=\frac{\hbar eF}{I_{1s}^2\sqrt{2mI_{1s}}}(I_{av,pv'}-I_{1s}-e\mathbf{F}\cdot\mathbf{R}_j)-\frac{\hbar eF}{I_{1s}\sqrt{2mI_{1s}}}-\frac{1}{2I_{1s}^2}(I_{av,pv'}-I_{1s}-e\mathbf{F}\vec{\cdot}\mathbf{R}_j)^2, \tag{2.40}$$

and

$$h_{j,1s,C}(I_{av,pv'})=\frac{\sqrt{2mI_{1s}}}{\hbar eF}\left(I_{av,pv'}-\frac{I_{1s}}{3}-e\mathbf{F}\cdot\mathbf{R}_j\right). \tag{2.41}$$

Next, it will be necessary to check the validity of the Condon approximation in deriving the above formulas. For this purpose, we consider the following simplest model system. The system considered is depicted in Fig. 2, where two identical harmonic oscillators for the neutral and ionized states are displaced from each other by ΔR. Under the Condon approximation, we have

$$\left|\langle\Theta_{pv'}|\Theta_{av}\rangle\right|^2\big|_{v=0} = \frac{S^{v'}e^{-S}}{v'!}, \tag{2.42}$$

where

$$S = \beta\Delta R^2/2, \quad \beta = \mu_{H_2}\omega_h/\hbar, \quad \text{and} \quad \omega_h = \sqrt{k_f/\mu_{H_2}} \tag{2.43}$$

for the transition from the vibrational state $v=0$ to the vibrational state v'. Here, S is the Huang-Rhys factor, μ_{H_2} the reduced mass of H_2, and k_f the force constant. The above formulas, Eqs. (2.28), (A6), and (2.38), using Eq. (2.42) are applicable for both the parallel and perpendicular laser polarization cases.

For the derivation of the ionization rate under the non-Condon approximation, we have only to change Eq. (2.27) to the following form:

$$\begin{aligned} I_{\mathrm{NC}}(\mathbf{k},\mathbf{R}_j,v=0,v') &= \langle\Theta_{pv'}|e^{i\mathbf{k}\cdot\mathbf{R}_j}|\Theta_{av}\rangle\big|_{v=0} \\ &= \frac{1}{\sqrt{v'}}\left(\frac{\beta}{2}\right)^{v'/2}\left(\Delta R - \frac{i(-1)^j}{2}\frac{\mathbf{k}\cdot\mathbf{R}}{\beta}\right)^{v'}\exp\left[-\frac{\beta}{4}\left\{\Delta R^2 + \left(\frac{\mathbf{k}\cdot\mathbf{R}}{2\beta}\right)^2\right\} + \frac{i}{2}(-1)^j\mathbf{k}\cdot(\mathbf{R}_{0a}+\Delta R\mathbf{R}/2)\right], \end{aligned} \tag{2.44}$$

where $\hat{\mathbf{R}}$ denotes the unit vector along $\hat{\mathbf{R}}_{0a}$ and it is also assumed that the initial vibrational state is $v=0$. On the other hand, under the Condon approximation, we have

$$I_C(\mathbf{k},\mathbf{R}_j,v=0,v') = \frac{1}{\sqrt{v'}}\left(\frac{\beta}{2}\right)^{v'/2}(\Delta R)^{v'}\exp\left\{-\frac{\beta}{4}\Delta R^2 + \frac{i}{2}(-1)^j\mathbf{k}\cdot\mathbf{R}_{0a}\right\}. \tag{2.45}$$

The difference between $I_C(\mathbf{k},\mathbf{R}_j,v,v')$ and $I_{\mathrm{NC}}(\mathbf{k},\mathbf{R}_j,v,v')$ is that the latter contains extra terms $-[i(-1)^j/2][(\mathbf{k}\cdot\hat{\mathbf{R}})/\beta]$ in the preexponential factor, and $-(\beta/4)[(\mathbf{k}\cdot\hat{\mathbf{R}})/2\beta]^2$ and $+(i/4)(-1)^j\Delta R\mathbf{k}\cdot\hat{\mathbf{R}}$ in the exponent.

Under the non-Condon approximation with the molecular axis parallel to the laser polarization, the individual photoionization rate $w^{j,1s,j,1s}_{av\to pv',\mathrm{NC,par}}$ is given by

$$w^{j,1s,j,1s}_{av\to pv',\mathrm{NC,par}} = \frac{(2^{v'}/v'!)E_{1s}|b_{j,1s}|^2|D_{j,1s,\mathrm{NC,par}}(I_{av,pv'})|^2\exp\{-2g^{(1)}_{\mathrm{har},j,1s}(I_{av,pv'})\}}{B_{j,1s,\mathrm{NC,par}}(I_{av,pv'})} \tag{2.46}$$

The definitions of the terms are given in Appendix B.

In Eq. (B9), the term $+(\beta/4)\Delta R^2$ is nothing but one of the factors of the Franck-Condon factor, e^{-S} in the Condon approximation, while the term $+[(-1)^j\sqrt{2mI_{1s}}/4\hbar]\Delta R - (mI_{1s}/8\hbar^2\beta)$ purely stems from the non-Condon approximation. The first term on the right-hand side (rhs) of Eq. (B9) is the same as that in the absence of the vibrational degrees of freedom. From this, we notice that including vibrational motion in molecules under the Condon approximation decreases photoionization rate by the Huang-Rhys factor $S/2=(\beta/4)\Delta R^2$, the inclusion of the vibrational motion under the non-Condon approximation further changes it by the factor $[(-1)^j\sqrt{2mI_{1s}}/4\hbar]\Delta R-(mI_{1s}/8\hbar^2\beta)$. Therefore, while keeping S constant, an increase of ΔR will bring about significant change of the photoionization rate in the non-Condon approximation using this factor; particularly for $j=2$, the ionization rate will decrease significantly.

In the preexponential factors defined by the equations from Eqs. (B1)–(B8), the terms

$$\frac{(-1)^j m\omega}{4\sqrt{2mI_{1s}}}\left\{\Delta R - \frac{(-1)^j\sqrt{2mI_{1s}}}{2\hbar\beta}\right\}$$

in Eq. (B1),

$$-\frac{\gamma_{1s}(eF)^2}{8\beta\hbar\omega} + (-1)^j eF\frac{\Delta R}{4}$$

in Eq. (B5), and $+m\omega/8\beta\hbar\gamma_{1s}^2$ in Eq. (B6), $-(-1)^j\gamma_{1s}(eF)/2\beta\hbar\omega$ in Eq. (B7), and $-(-1)^j\gamma_{1s}(eF)/4\beta\hbar\omega$ in Eq. (B8) also originate purely from the non-Condon approximation. Note that the term on the third line of the rhs of Eq. (B1) is independent of the Franck-Condon factor, and Condon and non-Condon approximations.

For v' larger than zero, we can compare Condon and non-Condon approximations. In the Condon approximation limit, $D_{j,1s,\mathrm{NC}}(I_{av,pv'})$ reduces to

$$D_{j,1s,\mathrm{NC}}(I_{av,pv'}) \to \frac{(-1)^{v'}}{2^{v'/2}}S^{v'/2}D_{j,1s,C}(I_{av,pv'}), \tag{2.47}$$

which means that the preexponential factors in the Condon approximation limit also reproduce those of the Condon approximation.

The quantum interference term under the non-Condon approximation with molecular axis parallel to the laser polarization, $w^{j,1s,j',1s}_{av\to pv',\mathrm{NC,par}}$, is given by

$$w^{j,1s,j',1s}_{av\to pv',\mathrm{NC,par}} = \frac{(2^{v'}/v'!)E_{1s}b_{j,1s}b_{j',1s}D_{j,1s,\mathrm{NC,par}}(I_{av,pv'})D_{j',1s,\mathrm{NC,par}}(I_{av,pv'})\exp\{-2g^{(1)}_{\mathrm{har},1s}(I_{av,pv'})\}}{B_{1s,\mathrm{NC,par}}(I_{av,pv'})}, \tag{2.48}$$

where

$$B_{1s,\mathrm{NC,par}}(I_{av,pv'}) = \left(\sinh^{-1}\gamma_{1s} + \frac{I_{av,pv'}-I_{1s}}{2I_{1s}}\frac{\gamma_{1s}}{\sqrt{1+\gamma_{1s}^2}} - \frac{m\omega}{8\hbar\beta}\right) \times\left\{\sinh^{-1}\gamma_{1s} - \frac{\gamma_{1s}}{\sqrt{1+\gamma_{1s}^2}} + \frac{I_{av,pv'}-I_{1s}}{2I_{1s}}\frac{\gamma_{1s}^3}{(1+\gamma_{1s}^2)^{3/2}}\right\}^{1/2} \tag{2.49}$$

and

$$g^{(1)}_{\mathrm{har},1s}(I_{av,pv'}) = \frac{1}{\hbar\omega}\left(\tilde{I}_{av,pv'}\sinh^{-1}\gamma_{1s} - \tilde{I}_{1s}\frac{\gamma_{1s}\sqrt{1+\gamma_{1s}^2}}{1+2\gamma_{1s}^2}\right) + \frac{\beta}{4}\Delta R^2 - \frac{mI_{1s}}{8\hbar^2\beta}, \tag{2.50}$$

where $j=1$ and $j'=2$, or $j=2$ and $j'=1$. Here, it should be noticed that in the quantum interference term the factor $[(-1)^j\sqrt{2mI_{1s}}/4\hbar]\Delta R$, which is present in the individual photoionization rate, is absent so that the quantum interference term will not be affected significantly by the drastic change of ΔR. The factors pertaining to the non-Condon approximation, especially those of the preexponential factors, Eqs. (B2)–(B4), are difficult to analyze so that we shall numerically investigate them later. In any case, it clearly shows that the displacement ΔR has to be included properly for the accurate calculation of the molecular ionization rate.

For the case in which the molecular axis is perpendicular to the laser polarization (the molecular axis is parallel to the y axis), the individual photoionization rate and quantum interference terms under the non-Condon approximation, $w^{1s,1s}_{av\to pv',\mathrm{NC,per}}$ and $w^{j,1s,j',1s}_{av\to pv',\mathrm{NC,per}}$, are presented in Appendix C. The total photoionization rates under the non-Condon approximation are given by simply replacing C in Eqs. (2.36) and (2.37) with NC.

In all the formulas presented above, it should be noted that the slopes in the log–log plot of the molecular photoionization rates versus laser intensity are not the same as those of the atomic photoionization rates or those of the molecular photoionization rates with the ionization potential being substituted by the molecular ionization potential in the atomic photoionization formulas. This is most easily recognized, for example, by inspection of Eq. (2.41):

$$h_{j,1s}(I_{av,pv'}) = \frac{\sqrt{2mI_{1s}}}{\hbar eF}\left(I_{av,pv'} - \frac{I_{1s}}{3} - e\mathbf{F}\cdot\mathbf{R}_j\right). \tag{2.51}$$

If it happens that $I_{av,pv'}$ is equal to I_{1s} and $\mathbf{F}\cdot\mathbf{R}_j$ is equal to zero (e.g., the molecular axis is perpendicular to the laser polarization) at the same time, Eq. (2.51) becomes

$$h_{j,1s} = \frac{2\sqrt{2mI_{1s}}}{3\hbar eF}I_0. \tag{2.52}$$

This is the same exponent as that of the hypothetical atom having the atomic ionization potential I_0 which is equal to $I_{av,pv'}$ or I_{1s}. In this case, we can also see that the preexponential factor is also almost the same as that of this hypothetical atom and we will observe a good agreement between the photoionization rates of the molecule of interest and the hypothetical atom. However, in the actual molecules, this will hardly happen. In reality, $I_{av,pv'}$ is not equal to I_{1s}, $\mathbf{F}\cdot\mathbf{R}_j$ is not equal to zero, and much worse, $I_{av,pv'}$ is not a fixed parameter. Instead, we have to sum up photoionization rates from each ionization potential $I_{av,pv'}$ as is shown in Eq. (2.37). This implies that great caution must be taken when applying the atomic photoionization rate formulas to the real molecules as was done in previous investigations.

In the numerical calculations shown below, we include the semiclassical Coulomb correction for the preexponential factors as was suggested by Keldysh [1],

$$\frac{I_{av,pv'}\gamma_{av,pv'}}{\hbar\omega\sqrt{1+\gamma_{av,pv'}{}^2}}, \tag{2.53}$$

for each vibrational excitation. In this case, we have different preexponential factors as shown in the following. That is, we have to substitute $E_{1s}(I_{av,pv'})$ and $E'_{1s}(I_{av,pv'})$ for E_{1s} and E'_{1s},

$$E_{1s}(I_{av,pv'}) = \frac{2\sqrt{2\pi}\gamma_{1s}^4\gamma_{av,pv'}}{\sqrt{1+\gamma_{av,pv'}{}^2}}\sqrt{\frac{I_{1s}I_{av,pv'}{}^2}{\hbar^3\omega}}, \tag{2.54}$$

$$E'_{1s}(I_{av,pv'}) = \frac{2^{17/4}\sqrt{3\pi}m^{5/4}I_{1s}{}^{13/4}I_{av,pv'}{}^{3/2}}{(eF)^{5/2}\hbar^{7/2}}, \tag{2.55}$$

and

$$\gamma_{av,pv'} = \frac{\omega\sqrt{2mI_{av,pv'}}}{eF}$$

(Keldysh parameter of the molecule). (2.56)

Here, we have explicitly shown that these factors depend on the vibrational excitations considered.

III. COMPUTATIONAL METHOD

A. *Ab initio* calculation

Ab initio quantum chemistry calculations are performed for the ground state of H_2 molecules. Its geometry is optimized using the hybrid density functional method B3LYP

with the 6-31G basis set and the corresponding harmonic frequencies are characterized at the same level of theory. From the force-constant matrix calculation, no vibrational modes with imaginary frequencies are found, which means that the truly local minimum has been obtained.

Using the optimized geometry calculated above, the molecular orbital coefficients $b_{j,1s}$ $(j=1,2)$ are obtained by the HF method with the STO-3G basis set. The package of GAUSSIAN 98 is employed for all the *ab initio* calculations performed in this work [17]. In this preliminary work, higher levels of *ab initio* calculations will not be carried out.

B. Calculation of Franck-Condon factors $|\langle\Theta_{pv'}|\Theta_{av}\rangle|^2$

The potential energy of the H_2 ground electronic state can analytically be represented by the following Morse potential:

$$V_a(R) = D_a[\exp\{-2\beta_a(R-R_{0a})\} - 2\exp\{-\beta_a(R-R_{0a})\}] - \Delta V_{ap}, \tag{3.1}$$

where $D_a=4.7$ (eV), $\beta_a=1.0338$ (bohr^{-1}), $R_{0a}=0.74168$(Å), and $V_{ap}=15.427$ (eV). On the other hand, σ_g and σ_u states of H_2^+ molecules are given by [18]

$$V_{p,\varepsilon}(R) = D_p[\exp\{-2\beta_p(R-R_{0p})\} - 2t_\varepsilon\exp\{-\beta_p(R-R_{0p})\}], \tag{3.2}$$

where $D_p=2.7925$ (eV), $\beta_p=0.72$ (bohr^{-1}), $R_{0p}=2.0$ (bohr), and

$$t_\varepsilon = \begin{cases} 1.0 & \text{for } \varepsilon=\sigma_g \\ -1.1 & \text{for } \varepsilon=\sigma_u. \end{cases} \tag{3.3}$$

The PECs are depicted in Fig. 3(a).

The transition dipole moments between the σ_g and σ_u states of H_2^+ molecules are calculated to obtain the field-modified PECs of H_2^+. The analytical expression is given by [18]

$$\mu(R) = \begin{cases} \mu + \dfrac{\mu'}{\beta_\varepsilon y}[1-\exp\{-\beta_\varepsilon y(R-R_{0_p})\}] & \text{for } R \leqslant 12 \text{ bohr} \\ R/2 & \text{for } R > 12 \text{ bohr}, \end{cases} \tag{3.4}$$

where $\mu=1.07$ (a.u.), $\mu'=0.396$ (a.u.), and $y=-0.055$.

The vibrational wave function $(v=0)$ of the ground electronic state of H_2 is given by the analytical eigenfunction of the Morse potential of $V_a(R)$. In addition, analytical eigenfunctions of the Morse potential $V_{p,\sigma_g}(R)$ are used. For the dissociative potential $V_{p,\sigma_u}(R)$, we only have continuum states: $\Theta_{p,E}(R)$. In order to obtain $\Theta_{p,E}(R)$, we numerically solve the following time-independent Schrödinger equation,

$$\left\{-\frac{\hbar^2}{2\mu_{H_2}}\frac{d^2}{dR^2} + V_{p,\sigma_u}(R)\right\}\Theta_{p,E}(R) = E\Theta_{p,E}(R) \tag{3.5}$$

using the shooting method [19]. We normalize the continuum eigenfunctions to satisfy

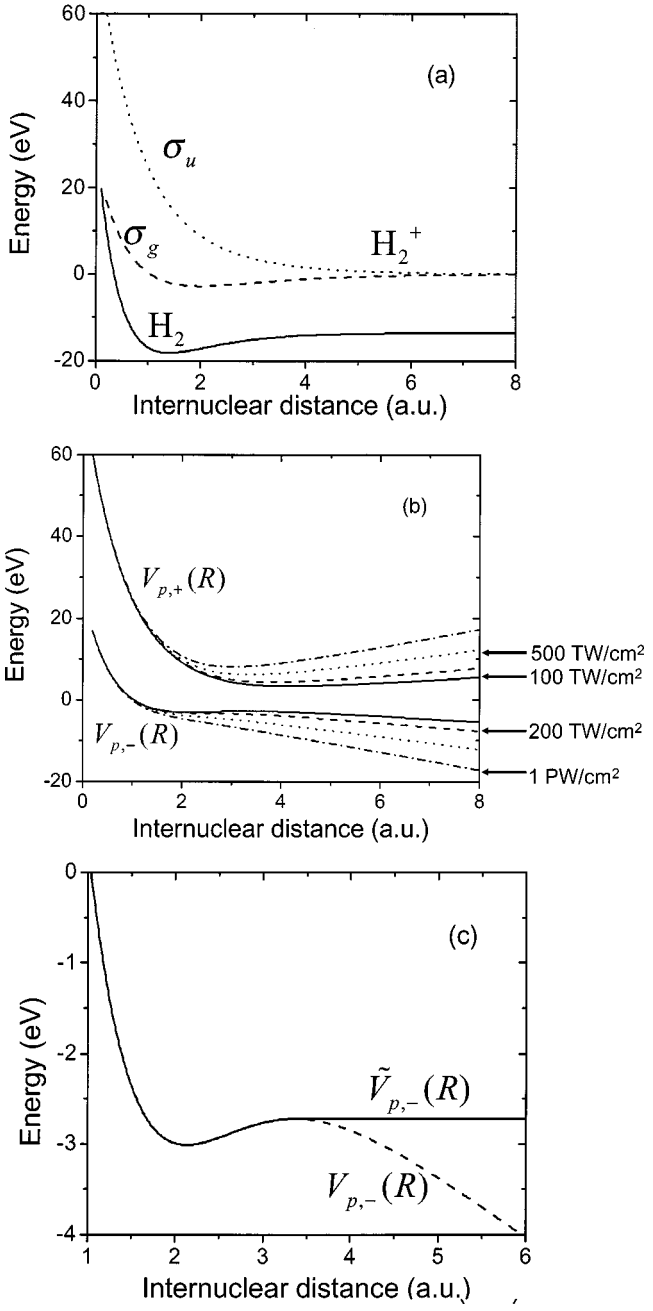

FIG. 3. Calculation results of PECs of H_2 and H_2^+ relevant to the present work. (a) Potential energy curves (PECs) of H_2 and H_2^+ molecules relevant to the tunneling ionization of theH_2 molecule. (b) Field-modified PECs $V_{p,\pm}(R)$ of the H_2^+ molecule. (c) Artificially cut PECs $\tilde{V}_{p,-}(R)$ and $V_{p,-}(R)$ of the H_2^+ molecule. The laser intensity is 100 TW/cm^2.

$$\int \Theta^*_{p,E'}(R)\Theta_{p,E}(R)dR = \delta(E-E'). \tag{3.6}$$

This normalization is done by ensuring that $\Theta_{p,E}(R)$ is equal to the Jordan-Wenzel-Kramers-Brillouin wave function

$$\left(\frac{2\mu_{H_2}}{\pi\hbar^2}\right)^{1/2}\frac{1}{k(x)^{1/2}}\sin\left(\int_{a_t}^{x}k(x)dx+\frac{\pi}{4}\right)$$

at some point far from the classical turning point $x=a_t$ where $k(x)=[2\mu_{H_2}\{E-V_{p,\sigma_u}(R)\}]^{1/2}/\hbar$ [20].

In the parallel laser polarization case, the PECs of H_2^+ are significantly modified by the laser field. In order to take into account this Stark shift, we have to diagonalize the following matrix:

$$\begin{bmatrix} V_{p,\sigma_g}(R) & -\mu(R)F \\ -\mu(R)F & V_{p,\sigma_u}(R) \end{bmatrix}. \tag{3.7}$$

Then we can obtain the field-modified adiabatic PECs $V_{p,-}(R)$ and $V_{p,+}(R)$:

$$V_{p,\pm}(R)=\frac{V_{p,\sigma_g}(R)+V_{p,\sigma_u}(R)}{2} \pm\sqrt{\left\{\frac{V_{p,\sigma_g}(R)-V_{p,\sigma_u}(R)}{2}\right\}^2+\{\mu(R)F\}^2}. \tag{3.8}$$

These adiabatic potentials are depicted in Fig. 3(b).

When the laser intensity exceeds 200 TW/cm^2, $V_{p,-}(R)$ becomes completely dissociative and does not have any discrete vibrational states. In this case, we calculate the continuum states $\Theta_{p,E}(R)$ in the same way as described above.

On the other hand, when the laser intensity is smaller than 200 TW/cm^2, $V_{p,-}(R)$ has several quasibound vibrational states. For the quasibound states with short lifetime, it is easy to obtain $\Theta_{p,E}(R)$ and to calculate $|\langle\Theta_{pv'}|\Theta_{av}\rangle|^2$ which shows a broad profile, while for those with very long lifetime, $|\langle\Theta_{pv'}|\Theta_{av}\rangle|^2$ shows a very steep and large peak, so that we require very small energy steps and much more computational time. To avoid this, we numerically calculate the discrete vibrational eigenstates for the potential cutoff artificially: $\tilde{V}_{p,-}(R)$ [see Fig. 3(c)]. It is numerically assured that $\Sigma_{v'}|\langle\tilde{\Theta}_{pv'}|\Theta_{av}\rangle|^2+\int dE|\langle\tilde{\Theta}_{p,E}|\Theta_{av}\rangle|^2$ is almost equal to unity (the percentage of the numerical errors is of the order of 0.1% for any laser intensities used in this work).

When the laser intensity becomes very large, $V_{p,+}(R)$ becomes a steep potential well and has dense discrete eigenstates. In this case, we calculate them numerically with the method described above. We can then determine the Franck-Condon factor $|\langle\Theta_{pv'}|\Theta_{av}\rangle|^2$. Strictly speaking, even when the laser intensity is low, $V_{p,+}(R)$ forms a bound PEC. Since this potential well is very shallow, we approximately regard the eigenstate as continuum and calculate the Franck-Condon factor $|\langle\Theta_{p,E}|\Theta_{av}\rangle|^2$ accordingly.

Although we did not take into account the field distortion of the ground state PEC of H_2 molecules, it is a reasonable first-order approximation [8].

IV. NUMERICAL RESULTS AND DISCUSSION

In this section, we show numerical results of the tunneling single-photoionization rate of a H_2 molecule calculated by using the formulas derived in Sec. III. The other factors, for example, the molecular orbital coefficients $b_{j,1s}$ and the quantities associated with PECs (the ionization potential $I_{av,pv'}$, the internuclear distance R_1-R_2, etc.) can only be obtained numerically so that the numerical values obtained in Sec. III will be used. In the numerical calculations for the comparison between the Condon and non-Condon approximations, the molecular orbital coefficients are assumed to be constant even if we are working with the parallel polarization case. In all of the calculations shown below, we assume that the initial vibrational state v is equal to zero. In addition, the semiclassical corrections, Eqs. (2.54) and (2.55), are used except for Fig. 6.

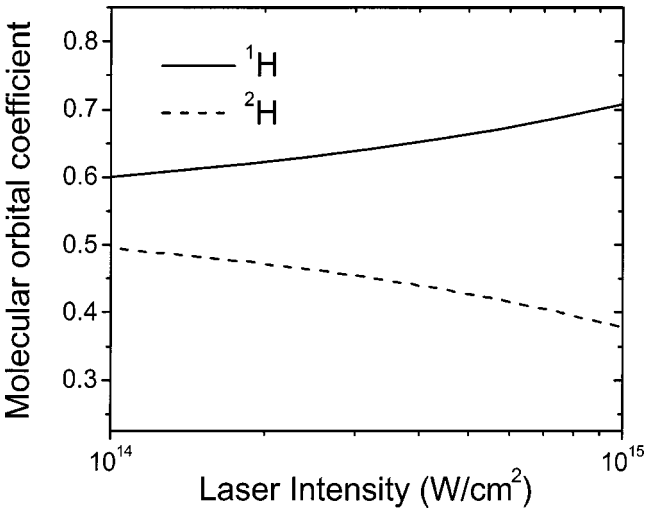

FIG. 4. Laser intensity dependence of the molecular orbital coefficients $b_{j,1s}$ $(j=1,2)$ of the ground electronic state of H_2 molecule calculated at the HF/STO-3G level of theory. The laser polarization is parallel to the molecular axis.

Figure 4 shows the molecular orbital coefficients $b_{j,1s}$ $(j=1,2)$ for the case of the parallel laser polarization. We can clearly see that $b_{1,1s}$ increases while $b_{2,1s}$ decreases with laser intensity due to the polarizability of the molecule. This is characteristic of the molecules in intense laser fields.

On the other hand, the molecular orbital coefficients $b_{j,1s}$ $(j=1,2)$ for the case of the perpendicular laser polarization are 0.548 36 in any laser field amplitudes. This value agrees with the analytical value very well.

Figure 5(a) shows the photoionization rate versus laser intensity in the tunneling limit when the laser polarization is parallel to the molecular axis. In this figure, we compare our results with those of Saenz calculated in *ab initio* fashion [Fig. 3(a) of Ref. [21]]. The comparison shows that the numerical results calculated seem to be reliable so that we can carry out benchmark tests. Another reason is that we do not yet have experimental data to compare with our calculation quantitatively (i.e., the absolute value of the photoionization rate). From the figure, we can see that our results reproduce Saenz's results well. In addition, we notice that the hydrogen atom ^{1}H, which is upstream along the laser polarization direction, contributes to the total photoionization predominantly. This is due to the fact that the exponential factor $\exp(2\sqrt{2mI_{1s}}\mathbf{F}\cdot\mathbf{R}_j/\hbar F)$ of ^{1}H is much larger than that of ^{2}H.

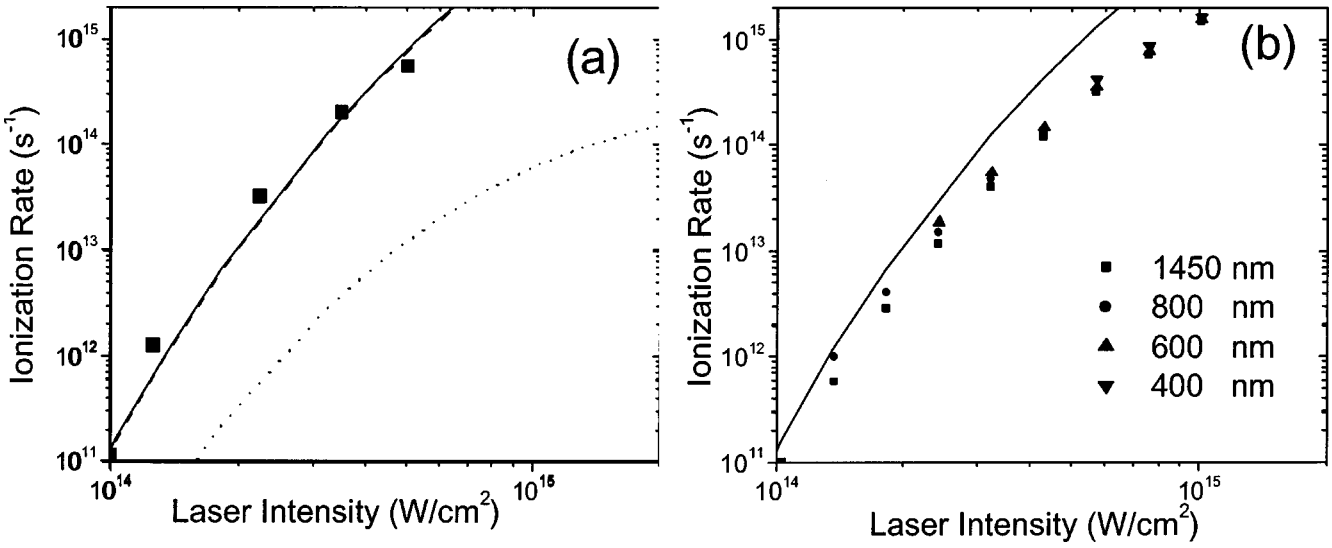

FIG. 5. Photoionization rates versus laser intensity of the H_2 molecule in the tunneling limit with the laser polarization parallel to the molecular axis, calculated by using Eq. (2.38) [panel (a)] and quantum interference terms for the laser wavelengths 1450, 800, 600, and 400 nm calculated by Eq. (A6) [panel (b)]. Panel (a) is compared with that calculated by the *ab initio* method [Fig. 3(a) of [21]]. In this panel, the solid squares stand for the results taken from Fig. 3(a) of [21], the solid line for the total photoionization rate calculated by Eq. (2.38), the broken line for the partial contribution from ^{1}H, and dotted line for that from ^{2}H of Fig. 1. Note that the solid and broken lines are superimposed in panel (a). This means that the total photoionization rate is dominated by that of ^{1}H in the parallel laser polarization case.

This is consistent with the results reported so far [22].

As mentioned in Sec. II, Eq. (2.38) does not include the quantum interference terms appropriately. We have to check if the total photoionization rate demonstrated in panel (a) (solid line) is reliable. Figure 5(b) shows the quantum interference terms for the laser wavelengths 1450, 800, 600, and 400 nm calculated by using Eq. (A6). It is found that as the laser wavelength increases, the quantum interference terms decrease. This tendency indicates that it is reasonable to assume that the quantum interference terms in the tunneling limit are smaller at least than those with the laser wavelength 1450 nm. Comparing panels 5(a) and 5(b), we can see that the quantum interference terms are several factors smaller than the individual and total photoionization rates. This fact leads to the conclusion that the quantum interference terms are negligibly smaller than the individual or total photoionization rates in the tunneling limit.

Figure 6 compares the total photoionization rates with and without the quasiclassical correction of the long-range Coulomb potential effect in the tunneling limit. We can see that if the correction is not included, the photoionization rate becomes about ten times lower than that with the correction. In general, the order of this difference becomes larger as the laser intensity decreases or $I_{av,pv'}$ increases since in the tunneling limit we have the semiclassical Coulomb correction $I_{av,pv'}\sqrt{2mI_{ac,pv'}}/\hbar eF$ from Eq. (2.53).

Figure 7 compares the total photoionization rates with and without the Franck-Condon factors. The difference between these two cases is not negligible, twice or thrice larger for the case without Franck-Condon factor. However, we can see a slight tendency that the inclusion of the Franck-Condon factors causes decrease of the photoionization rate, which is consistent with that calculated by the ADK formula [8].

Figure 8 shows the photoionization rate versus laser intensity when the laser polarization is perpendicular to the molecular axis. Comparing Figs. 5 and 8, we can see that the photoionization rate with the perpendicular laser polarization is much smaller than that with the parallel laser polarization. In addition, we notice that the partial contributions from ^{1}H and ^{2}H hydrogen atoms are of the same magnitude. This can be easily understood by inspection of Eqs. (2.38)–(2.41). In the perpendicular laser polarization, $\mathbf{F}\cdot\mathbf{R}_j$ for both $j=1$ and $j=2$ is zero so that $w^{j,1s,j,1s}_{av\to pv',C,\mathrm{Tun}}$ is identical for both $j=1$ and $j=2$. This comparison between the parallel and

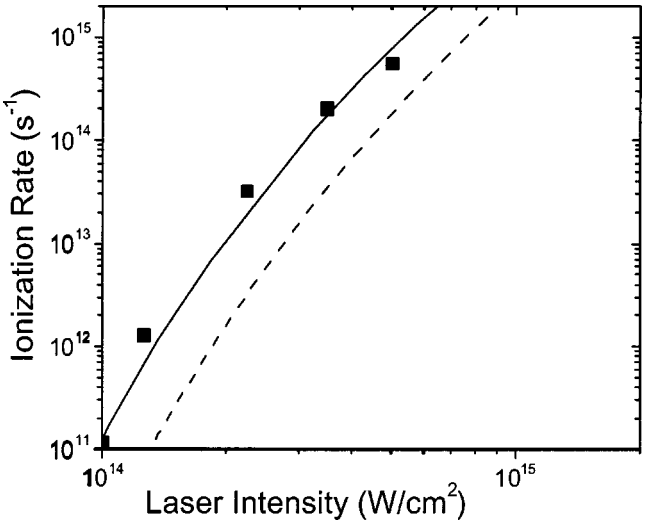

FIG. 6. Comparison of the photoionization rates versus laser intensity of H_2 molecule in the tunneling limit with semiclassical correction and without it. The solid line and the squares are the same as those in Fig. 5 while the broken line is calculated under the assumption of no correction. This figure indicates the importance of the Coulomb correction for the accurate calculation of the photoionization rates.

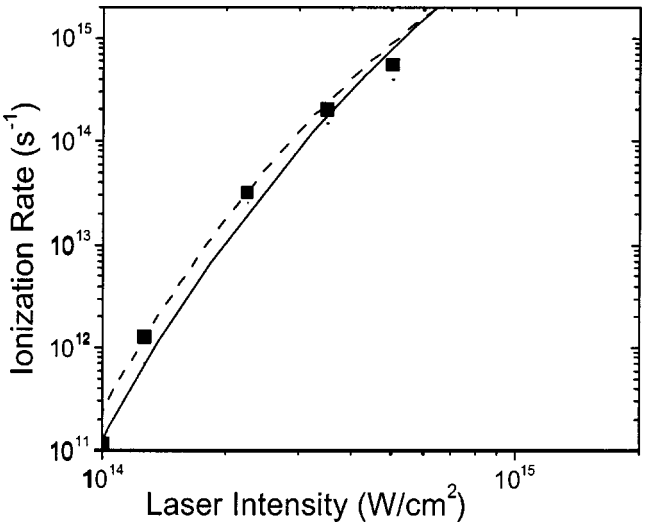

FIG. 7. Comparison between the molecular photoionization rates, including the Franck-Condon factor, and those in its absence i.e., only the photoionization rate of the transition to the vibrational level $v'=0$ is considered.). The solid line and the squares are the same as those in Fig. 5 while the broken line is calculated under the assumption of no Franck-Condon factors.

perpendicular laser polarization cases actually indicate the importance of the site-dependent exponential factor of $\exp(2\sqrt{2mI_{1s}}\mathbf{F}\cdot\mathbf{R}_j/\hbar F)$.

In Table I, we show the laser frequency dependence of the total photoionization rates $w_{a,v,C}$ with the parallel laser polarization under the Condon approximation. We can see that increasing the laser frequency leads to the enhancement of the total photoionization rate provided that the laser intensities are identical. The frequency dependence of the photoionization rates can be analyzed more conveniently by the Keldysh type of theories than by ADK theory since the laser

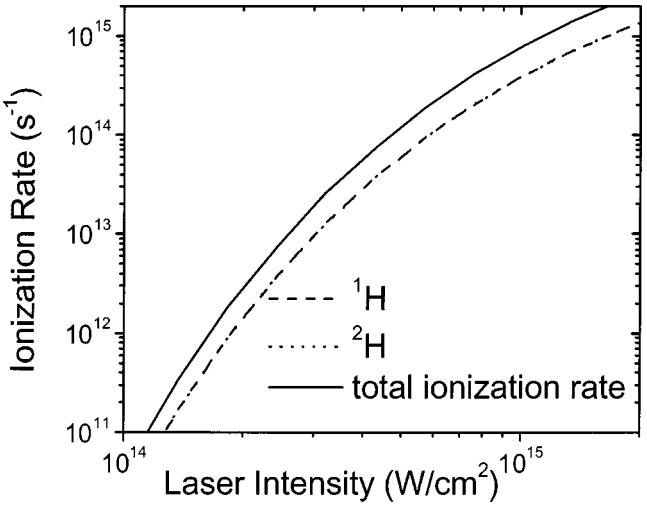

FIG. 8. Photoionization rates versus the laser intensity of the H_2 molecule in the tunneling limit, with the laser polarization perpendicular to the molecular axis, calculated by using Eq. (2.38). The broken and dotted lines are the partial photoionization rates from ^{1}H and ^{2}H, respectively. The solid line is for the total photoionization rate. Note that the broken and dotted lines are superimposed.

frequency dependence cannot be included in an explicit fashion in the latter case.

So far, the Condon approximation was assumed. Below, we shall investigate the validity of the Condon approximations made in the above discussion. In the following calculations for the comparison between the Condon and non-Condon approximations, the parameters are chosen to be laser intensity 7.59×10^{14} (W/cm^2), $\omega=1.55$ (eV) [or wavelength=800 (nm)], $R_{0a}=0.735$ (Å) (very close to the equilibrium distance of the H_2 molecule in the electronic ground state), and $\Delta E=17.33$ (eV).

Figure 9 shows that Huang-Rhys factor S defined by Eq. (2.43) with the parameters defined above. We can see that as far as both parameters β and ΔR are very small, the Huang-Rhys factor is very small, which is reasonable in real systems. However, if these parameters are very large, the most probable vibrational excitation is to the higher vibrational states of the ionic potential.

Figures 10 and 11 compare the molecular ionization rates under the Condon and non-Condon approximations for the cases of the parallel and perpendicular polarizations, respectively. In the case of the perpendicular polarization, we can see the good agreement between the results under the Condon and non-Condon approximations; in particular, the photoionization rate with the perpendicular laser polarization is much more insensitive to the Condon approximation. In the linear laser polarization case, we can see around a ten times difference between the Condon and non-Condon approximations (from Fig. 10). In addition, we notice that as β or ΔR becomes small, the total photoionization rate becomes larger. This is due to that fact that in this case the quantum number of the vibrational state of the ionic state with the largest Franck-Condon factor is $v'=0$. In addition, the transition to the state $v'=0$ has the smallest ionization potential $I_{av,pv'}$. Since the photoionization rate is very sensitive to the value of $I_{av,pv'}$ but less sensitive to the Franck-Condon factor, the transition to the state $v'=0$, which has the largest Franck-Condon factor, has the largest photoionization rate in all the situations. From the figures, we can see that the photoionization rates seem to be more sensitive to β than to ΔR.

In the area where the Condon and non-Condon approximations do not agree well, the photoionization rates under the non-Condon approximation are larger than those under the Condon approximation because of the several times difference of the exponential and preexponential factors. In addition, due to the lack of the term $(\sqrt{2mI_{1s}}/2h)(-1)^j R_{0a}$ in the exponent in the quantum interference terms, the contribution from the quantum interference term is smaller by one or three orders of magnitude than the individual photoionization rate contributed from ^{1}H.

Finally, we note the recently published work concerning the experimental results of vibrational distribution of H_2^+ molecule in the tunneling photoionization of the process of Eq. (2.13) [23]. This study has clearly demonstrated the importance of including the vibrational degrees of freedom for the molecular tunneling photoionization. They have found that the relative populations of the vibrational states of H_2^+ molecule after the tunneling photoionization of H_2 molecule do not follow the conventional Franck-Condon principle.

TABLE I. Total photoionization rate (s^{-1}) of H_2 to H_2^+ for various laser wavelengths when the laser polarization is parallel to the molecular axis.

Wavelength λ(nm) laser intensity γ_{1s}	Tunneling limit	1450	γ_{1s}	800	γ_{1s}	600	γ_{1s}	400	γ_{1s}
1.03×10^{14}	1.62×10^{11}	3.58×10^{11}	0.58						
1.37×10^{14}	1.14×10^{12}	2.13×10^{12}	0.50	3.74×10^{12}	0.91				
1.82×10^{14}	6.57×10^{12}	1.09×10^{13}	0.44	1.62×10^{13}	0.79				
2.43×10^{14}	3.21×10^{13}	4.74×10^{13}	0.38	6.21×10^{13}	0.68	8.03×10^{13}	0.91		
3.23×10^{14}	1.23×10^{14}	1.74×10^{14}	0.33	2.10×10^{14}	0.59	2.51×10^{14}	0.79		
4.29×10^{14}	4.20×10^{14}	5.64×10^{14}	0.28	6.39×10^{14}	0.51	7.25×10^{14}	0.69		
5.71×10^{14}	1.27×10^{15}	1.63×10^{15}	0.25	1.78×10^{15}	0.45	1.94×10^{15}	0.60	2.40×10^{15}	0.89
7.60×10^{14}	3.49×10^{15}	4.29×10^{15}	0.21	4.53×10^{15}	0.39	4.81×10^{15}	0.52	5.59×10^{15}	0.77
1.01×10^{15}	8.84×10^{15}	1.05×10^{16}	0.19	1.09×10^{16}	0.34	1.13×10^{16}	0.45	1.25×10^{16}	0.67
1.34×10^{15}	2.12×10^{16}	2.43×10^{16}	0.16	2.48×10^{16}	0.29	2.55×10^{16}	0.39	2.72×10^{16}	0.58

The reason for this is the rapid variation of the photoionization rate with the internuclear distance. They used the following formula to calculate the transition rates to the individual field-modified vibrational levels of H_2^+ molecules,

$$\Gamma(v') = \left| \int \Gamma^{1/2}(R)\chi_{v'}(R)\chi_0(R)dR \right|^2, \qquad (4.1)$$

where $\chi_{v'}(R)$ and $\chi_0(R)$ are the vibrational wave functions of H_2^+ and H_2 molecules, respectively, and $\Gamma(R)$ is the photionization rate dependent on the internuclear distance R. The R-dependent photoionization rate $\Gamma(R)$ is calculated by the ADK formula [4].

We compare their results to those obtained by our formulas. The relative population $p_{\mathrm{rel}}(v')$ in the vibrational state v' is given by

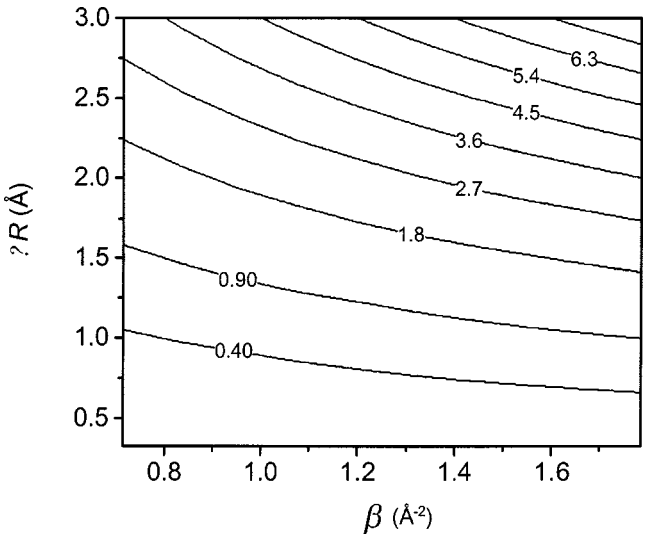

FIG. 9. Huang-Rhys factor S defined by Eq. (2.40) when the laser intensity is equal to 7.59×10^{14} (W/cm^2), ω=1.55 (eV) [or wavelength=800 (nm)], R_{0a}=0.735 (Å), and ΔE=17.33 (eV). The value on each curve represents S.

$$p_{\mathrm{rel}}(v') = \frac{w_{av\to pv',C}}{w_{av,C}} \qquad (4.2)$$

Figure 12 shows the relative populations for each vibrational state v' for the parallel and perpendicular laser polarization cases. As in [23], when the laser intensity is very large, the number of the bound or quasi-bound vibrational states of H_2^+ diminishes so that the total populations of the bound or quasibound vibrational states of H_2^+ decrease. For example, the total populations from the bound or quasibound states add up to 94%, 91%, and 70% for the Figs. 12(a)–12(c), respectively. This agrees well with the experimental results reported in the literature [23]. Contrary to the results obtained by Urbain *et al.* [23], the relative populations calculated in this work follow the same distributions predicted by Franck-Condon factors, although they claim that the dissociative photoionization does not follow the Franck-Condon principle since the ADK photoionization rate is dependent on R.

Some features are very similar between Fig. 2 of [23] and Fig. 12 of this work. For example, we notice that as the laser intensity increases, the relative populations of higher vibrational quantum number v' becomes larger for the perpendicular laser polarization case. This tendency agrees well with that of Figs. 2 and 4 of the literature [23].

From the above comparisons, we can conclude that if the laser intensity is very large, the prediction by the ADK theory and that of our theory are very similar. But if the laser intensity is not so large, these two theories yield very different results. The decisive conclusion has to await more experimental studies of intense laser ionization of different molecules.

V. CONCLUDING REMARKS

In this work, we have obtained the analytical Keldysh-type expressions for the photoionization rates of H_2 molecules in the linearly polarized electric field in the tunneling region. For this purpose, we have extended the Keldysh theory improved by us in previous works; especially, we

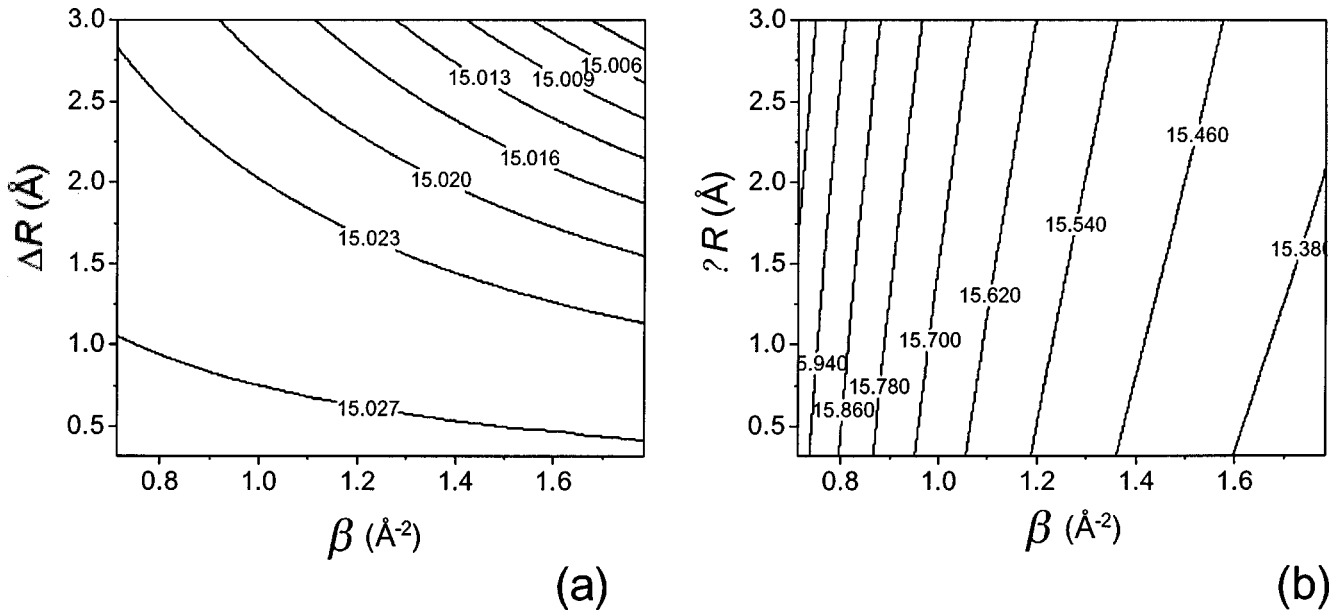

FIG. 10. Dependence of the total photoionization rates on β and ΔR with the same parameters used in Fig. 9 in the case of the parallel laser polarization. The value on each curve represents $\log_{10}$(total ionization rate in W/cm^2). In (a) and (b), the Condon and non-Condon approximations are assumed, respectively.

have included Franck-Condon factors to take the molecular vibrational degrees of freedom into consideration The comparison of the numerical calculations performed by using these formulas with the numerical results calculated by Saenz [21] has actually shown the validity of our formulas. Clearly, our formulas have more complicated structures than the ADK theory, but we could obtain physical insights from inspection of the formulas themselves and the numerical results. This feature is due to the simple structure of the formulas derived by the Keldysh-type theory: our formulas are expressed in the form of a combination of the exponential and preexponential terms, which is very similar to the original atomic Keldysh theory. However, in the case of molecules, there exists a special feature due to the interferences between different atoms. The explicit dependence of the photoionization rate on the laser frequency is also one of the advantages over other tunneling theories, e.g., the ADK theory.

We have only concentrated on the hydrogen molecule in the present paper. However, it is an easy task to extend the present procedures to other molecules whose molecular orbitals consist of the atomic orbitals such as $2s, 2px, 2py, 2pz$,

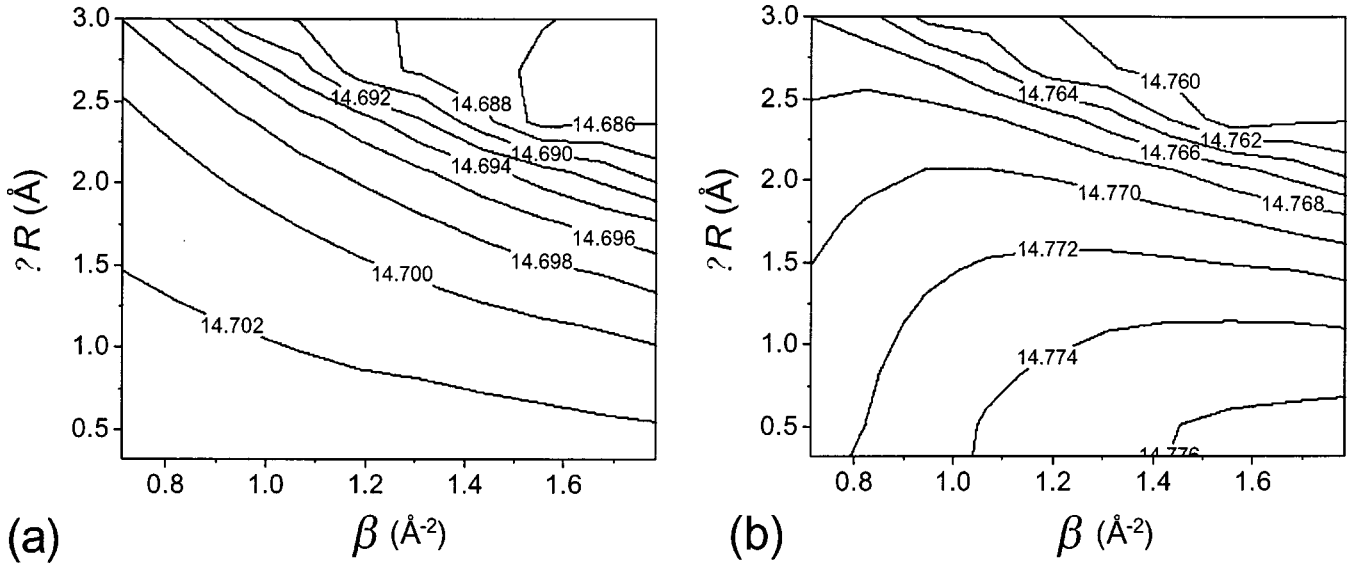

FIG. 11. Dependence of the total photoionization rates on β and ΔR with the same parameters used in Fig. 9 in the case of the perpendicular laser polarization. The value on each curve represents $\log_{10}$(total ionization rate in W/cm^2). In (a) and (b), the Condon and non-Condon approximations are assumed, respectively.

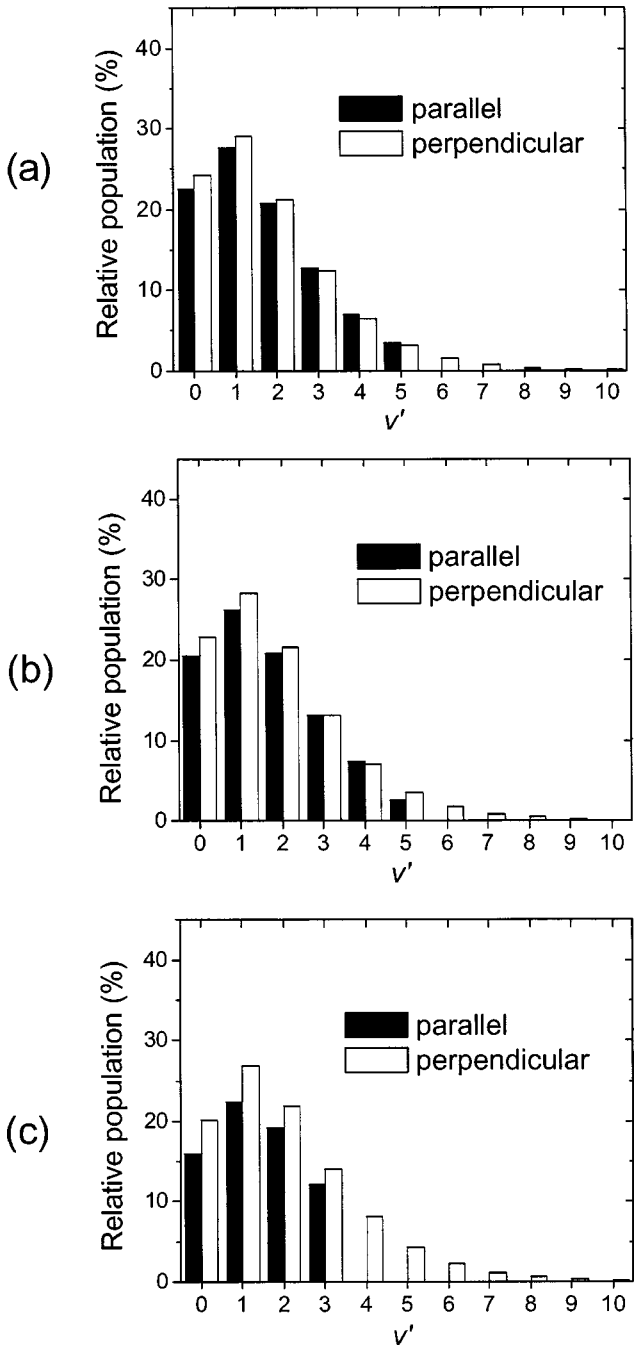

FIG. 12. Vibrational distributions of the H_2^+ molecule after the tunneling photoionization of the H_2 molecule. The laser intensities are (a) 4.4×10^{13}, (b) 5.84×10^{13}, and (c) 1.03×10^{14} (W/cm^2). These figures should be compared with Figs. 2 and 4 of the literature [23].

etc. (e.g., polyatomic organic molecules) in a similar way as the ADK expressions of the tunneling ionization rate of arbitrary complex atoms and atomic ions [4].

For large polyatomic molecules, unless the molecular axis is perpendicular to the laser polarization, the exponential factor pertaining to the molecules, $\exp(2\sqrt{2mI_{1s}}\mathbf{F}\cdot\mathbf{R}_j/\hbar F)$, will be large so that very different photoionization rates for the molecule and the atom with the identical ionization potential will be found; the same conclusion has been deduced by other authors [22]. However, the comparison between the numerical results obtained under the Condon and non-Condon approximations has shown that the exponent, $+[(-1)^j\sqrt{2mI_{1s}}/4\hbar]\Delta R-(mI_{1s}/8\hbar^2\beta)$, in Eq. (B9) also plays an important role for determining the photoionization rate if the molecular axis is parallel to the laser polarization. Again, this indicates the importance of properly including the vibrational degrees of freedom for the analysis of the molecular photoionization processes. This feature will be more noticeable for large polyatomic molecules, which must await experiments that are carried out for this purpose.

An important feature of the Keldysh-type theory is that it provides the absolute magnitude of photoionization rates. This information is important when there exist other photophysical processes competing with photoionization.

ACKNOWLEDGMENT

The authors wish to thank Academia Sinica, National Science Council of ROC for supporting this work.

APPENDIX A: DERIVATION OF THE QUANTUM INTERFERENCE TERMS

The quantum interference terms are derived as follows: from Eq. (2.25), we obtain

$$w^{j,1s,j',1s}_{av\to pv',C}=\frac{4\pi}{\hbar}\mathrm{Re}\Bigg[b^*_{j,1s}b_{j,1s}C^*_{1s}C_{1s}D^*_{j,1s}(I_{av,pv'})D_{j',1s}(I_{av,pv'})\times|\langle\Theta_{pv'}|\Theta_{av}\rangle|^2\exp\{-g^{(1)}_{j,1s,C}(I_{av,pv'},\mathbf{R}_j)-g^{(1)}_{j',1s,C}\times(I_{av,pv'},\mathbf{R}_{j'})\}\int\frac{d^3p}{(2\pi\hbar)^3}\exp\Bigg[\frac{i}{\hbar}(\mathbf{R}_j-\mathbf{R}_{j'})\cdot\mathbf{p}-i\{g^{(2)}_{j,1s}(I_{av,pv'})-g^{(2)}_{j',1s}(I_{av,pv'})\}p\cos\theta_p-\{g^{(3)}_{j,1s}\times(I_{av,pv'})+g^{(3)}_{j',1s}(I_{av,pv'})\}p^2-\{g^{(4)}_{j,1s}(I_{av,pv'})+g^{(4)}_{j',1s}(I_{av,pv'})\}p^2\cos^2\theta_p\Bigg]\sum_{n=-\infty}^{\infty}\delta\Bigg(\tilde{I}_{av,pv'}+\frac{p^2}{2m}-n\hbar\omega\Bigg)\Bigg],\tag{A1}$$

where

$$g^{(2)}_{j,1s}(I_{av,pv'})=\frac{1}{\hbar\omega}\Bigg\{\frac{eF}{m\omega}(1-\sqrt{1+\gamma_{1s}^2})-(I_{av,pv'}-I_{1s})\times\frac{\gamma_{1s}}{\sqrt{2mI_{1s}}\sqrt{1+\gamma_{1s}^2}}+\frac{e\mathbf{F}\cdot\mathbf{R}_j\gamma_{1s}}{\sqrt{2mI_{1s}}}\Bigg\},\tag{A2}$$

$$g^{(3)}_{j,1s}(I_{av,pv'})=\frac{1}{2m\hbar\omega}\Bigg\{\sinh^{-1}\gamma_{1s}+\frac{I_{av,pv'}-I_{1s}}{2I_{1s}}\frac{\gamma_{1s}}{\sqrt{1+\gamma_{1s}^2}}-\frac{e\mathbf{F}\cdot\mathbf{R}_j\gamma_{1s}}{2I_{1s}}\Bigg\},\tag{A3}$$

$$g^{(4)}_{j,1s}(I_{av,pv'}) = \frac{1}{2m\hbar\omega}\left\{ -\frac{\gamma_{1s}}{\sqrt{1+\gamma_{1s}^2}} - \frac{I_{av,pv'} - I_{1s}}{2I_{1s}}\frac{\gamma_{1s}}{(1+\gamma_{1s}^2)^{3/2}} + \frac{e\mathbf{F}\cdot\mathbf{R}_j\gamma_{1s}}{2I_{1s}}\right\}, \quad \text{(A4)}$$

and

$$C_{1s} = -\frac{2\sqrt{\pi}(2mI_{1s})^{5/4}\hbar^{3/2}\omega^2}{me^2F^2} \quad \text{(A5)}$$

Integrating over p, we finally obtain the general quantum interference terms for the homonuclear diatomic molecules consisting of only 1s atomic orbitals:

$$w^{j,1s,j',1s}_{av\to pv',C} = -\sqrt{\frac{\omega I_{1s}}{\pi\hbar}}\gamma_{1s}^4 b_{j,1s}b_{j',1s} \times D_{j,1s,C}(I_{av,pv'})D_{j',1s,C}(I_{av,pv'})|\langle\Theta_{pv'}|\Theta_{av}\rangle|^2 \times \exp\{-g^{(1)}_{j,1s,C}(I_{av,pv'},\mathbf{R}_j) - g^{(1)}_{j',1s,C}(I_{av,pv'},\mathbf{R}_{j'})\} \times \int d\Omega_p \frac{J^2_{j,1s,j',1s}(I_{av,pv'},\hat{\mathbf{p}}) - 2G_{1s,1s}(I_{av,pv'},\theta_p)}{G^{5/2}_{1s,1s}(I_{av,pv'},\theta_p)} \times\exp\left\{-\frac{J^2_{j,1s,j',1s}(I_{av,pv'},\hat{\mathbf{p}})}{4G_{1s,1s}(I_{av,pv'},\theta_p)}\right\}, \quad \text{(A6)}$$

where

$$j = 1 \text{ and } j' = 2, \text{ or } j = 2 \text{ and } j' = 1, \quad \text{(A7)}$$

$$G_{1s,1s}(I_{av,pv'},\theta_p) = 2m\hbar\omega\left[g^{(3)}_{j,1s}(I_{av,pv'}) + g^{(3)}_{j',1s}(I_{av,pv'})\left\{g^{(4)}_{j,1s} \times (I_{av,pv'}) + g^{(4)}_{j',1s}(I_{av,pv'})\right\}\cos^2\theta_p\right], \quad \text{(A8)}$$

$$J_{j,1s,j',1s}(I_{av,pv'},\hat{\mathbf{p}}) = \sqrt{\frac{2m\omega}{\hbar}}(\mathbf{R}_j - \mathbf{R}_{j'})\cdot\hat{\mathbf{p}} + \cos\theta_p\left\{K_{j,1s}(I_{av,pv'}) - K_{j',1s}(I_{av,pv'})\right\}, \quad \text{(A9)}$$

and

$$K_{j,1s}(I_{av,pv'}) = \frac{\gamma_{1s}}{\sqrt{\hbar\omega I_{1s}}}\left(\frac{I_{av,pv'} - I_{1s}}{\sqrt{1+\gamma_{1s}^2}} - e\mathbf{F}\cdot\mathbf{R}_j\right), \quad \text{(A10)}$$

and $\hat{\mathbf{p}}$ is the unit vector defined by $\mathbf{p}$. In this derivation, we have used the fact that $b_{j,1s}$, C_{1s}, and $D_{j,1s,C}(I_{av,pv'})$ are real. It is clear from Eqs. (A8)–(A10) that the quantum interference terms arise from the two-center geometry of the nuclear field: Only two different jth and j'th atoms contribute to each quantum interference term $w^{j,1s,j',1s}_{av\to pv',C}$. In particular, $J_{j,1s,j',1s}(I_{av,pv'},\hat{\mathbf{p}})$ depends on the distance between jth and j'th atoms while $G_{1s,1s}(I_{av,pv'},\theta_p)$ on the sum of the distances between jth and j'th atoms from the molecular center.

Because many terms which depend on the nuclear position cancel out in Eq. (A8) or completely disappear in the exponent in Eq. (A6) for the homonuclear diatomic molecules the quantum interference terms are less sensitive to molecular geometries than the individual photoionization rates for such a simple diatomic molecule.

APPENDIX B: DEFINITIONS OF THE TERMS IN EQ. (2.46)

The definitions of the terms appearing in Eq. (2.46) are given by

$$B_{j,1s,\mathrm{NC,par}}(I_{av,pv'}) = \left[\sinh^{-1}\gamma_{1s} + \frac{I_{av,pv'} - I_{ls}}{2I_{1s}}\frac{\gamma_{1s}}{\sqrt{1+\gamma_{1s}^2}} + (-1)^j eF\frac{R_{0a}}{2}\frac{\gamma_{1s}}{2I_{1s}} + \frac{(-1)^j m\omega}{4\sqrt{2mI_{1s}}}\left\{\Delta R - \frac{(-1)^j\sqrt{2mI_{1s}}}{2\hbar\beta}\right\}\right]\left\{\sinh^{-1}\gamma_{1s} - \frac{\gamma_{1s}}{\sqrt{1+\gamma_{1s}^2}} + \frac{I_{av,pv'} - I_{1s}}{2I_{1s}}\frac{\gamma_{1s}^3}{(1+\gamma_{1s}^2)^{3/2}}\right\}^{1/2}, \quad \text{(B1)}$$

$$D_{j,1s,\mathrm{NC,par}}(I_{av,pv'})_{v'=0} = \frac{X_{1,j}(I_{av,pv'})_{v'=0}}{\gamma_{1s}I_{1s}} - X_2(I_{av,pv'})_{v'=0} - \frac{X_{1,j}(I_{av,pv'})^2_{v'=0}}{2\hbar\omega I_{1s}} \quad \text{(B2)}$$

or

$$D_{j,1s,\mathrm{NC,par}}(I_{av,pv'})_{v'=1} = \frac{(-1)^j eF}{4\gamma_{1s}I_{1s}\sqrt{\beta}} + \frac{\sqrt{\beta}X_{1,j}(I_{av,pv'})_{v'=1}}{\gamma_{1s}I_{1s}}X_{3,j} - \left\{X_2(I_{av,pv'})_{v'=1} + \frac{X_{1,j}(I_{av,pv'})^2_{v'=1}}{2\hbar\omega I_{1s}}\right\}\sqrt{\beta}X_{4,j}, \quad \text{(B3)}$$

or

$$D_{j,1s,\mathrm{NC,par}}(I_{av,pv'})_{v'\geq 2} = \frac{v'(-1)^j eF\beta^{v'/2-1}}{4\gamma_{1s}I_{1s}}X_{4,j}^{v'-1} - \frac{v'(v'-1)(eF)^2\beta^{v'/2-2}}{32\hbar\omega I_{1s}}X_{4,j}^{v'-2} + \frac{\beta^{v'/2}(eF)X_{1,j}(I_{av,pv'})}{\omega\gamma_{1s}I_{1s}}\left\{X_{4,j}^{v'} - \frac{v'(-1)^j(eF)\gamma_{1s}}{4\beta\hbar\omega}X_{4,j}^{v'-1}\right\} - \beta^{v'/2}\left\{X_2(I_{av,pv'}) + \frac{X_{1,j}(I_{av,pv'})^2}{2\hbar\omega I_{1s}}\right\}X_{4,j}^{v'}, \quad \text{(B4)}$$

$$X_{1,j}(I_{av,pv'}) = \frac{I_{av,pv'} - I_{1s}}{\sqrt{1+\gamma_{1s}^2}} + (-1)^j eF\frac{R_{0a}}{2} - \frac{\gamma_{1s}(eF)^2}{8\beta\hbar\omega} + (-1)^j eF\frac{\Delta R}{4}, \quad \text{(B5)}$$

$$X_2(I_{av,pv'}) = \frac{1}{\gamma_{1s}\sqrt{1+\gamma_{1s}^2}} + \frac{(I_{av,pv'} - I_{1s})}{2I_{1s}} \frac{\gamma_{1s}}{(1+\gamma_{1s}^2)^{3/2}} + \frac{m\omega}{8\beta\hbar\gamma_{1s}^2} \tag{B6}$$

$$X_{3,j} = -\frac{\Delta R}{2} - \frac{(-1)^j \gamma_{1s}(eF)}{2\beta\hbar\omega}, \tag{B7}$$

,

$$X_{4,j} = -\frac{\Delta R}{2} - \frac{(-1)^j \gamma_{1s}(eF)}{4\beta\hbar\omega}, \tag{B8}$$

and

$$g^{(1)}_{\mathrm{har}j,1s}(I_{av,pv'}) = \frac{1}{\hbar\omega}\left(\tilde{I}_{av,pv'}\sinh^{-1}\gamma_{1s} - \tilde{I}_{1s}\frac{\gamma_{1s}\sqrt{1+\gamma_{1s}^2}}{1+2\gamma_{1s}^2}\right) + \frac{\sqrt{2mI_{1s}}}{2\hbar}(-1)^j R_{0a} + \frac{\beta}{4}\Delta R^2 + \frac{(-1)^j\sqrt{2mI_{1s}}}{4\hbar}\Delta R - \frac{mI_{1s}}{8\hbar^2\beta} \tag{B9}$$

for the homonuclear diatomic molecules.

APPENDIX C: TOTAL PHOTOIONIZATION RATE WITH THE PERPENDICULAR POLARIZATION UNDER THE NON-CONDON APPROXIMATION

The individual photoionization rate with the perpendicular polarization under the non-Condon approximation is given by

$$w^{j,1s,j,1s}_{av\to pv',\mathrm{NC,per}} = E_{1s}|b_{j,1s}|^2|D_{j,1s,C}(I_{av,pv'})|^2|\langle\Phi_{pv'}|\Phi_{av}\rangle|^2 \times\exp\{-2g^{(1)}_{j,1s,C}(I_{av,pv'},\vec{\mathbf{0}})\} \times\sum_{\lambda=0}^{v'}{}_{v'}C_\lambda \frac{(2\lambda+1)!!}{2^{3\lambda+3/2}\pi}\left(\frac{m\omega}{\hbar\beta^2\Delta R^2}\right)^\lambda \times\int_0^\pi \sin\theta d\theta\int_0^{2\pi} d\phi\left\{\eta_1 + \eta_2\cos^2\theta + \frac{m\omega}{8\hbar\beta}\sin^2\theta\sin^2\phi\right\}^{-(2\lambda+3)/2}, \tag{C1}$$

while the quantum interference terms are given by

$$w^{j,1s,j',1s}_{av\to pv',\mathrm{NC,per}} = E_{1s}b_{j,1s}b_{j',1s}|D_{j,1s,C}(I_{av,pv'})|^2|\langle\Phi_{pv'}|\Phi_{av}\rangle|^2 \times\exp\{-2g^{(1)}_{j,1s,C}(I_{av,pv'},\mathbf{0})\} \times\sum_{\lambda=0}^{v'}\sum_{\lambda'=0}^{v'}{}_{v'}C_{\lambda_{v'}}C_{\lambda'}(-1)^{j\lambda+j'\lambda'+\lambda'} \times\frac{1}{2^{\lambda+\lambda'}\pi^{3/2}}\left(\frac{m\omega}{\hbar\beta^2\Delta R^2}\right)^{(\lambda+\lambda')/2} \times\int_0^\pi d\theta(\sin\theta)^{\lambda+\lambda'+1}\int_0^{2\pi} d\phi(\sin\phi)^{\lambda+\lambda'} \times\mathrm{Re}[i^{\lambda+\lambda'}\Xi_{j,j'}(\lambda+\lambda',\theta,\phi)], \tag{C2}$$

where

$$\eta_1 = \sinh^{-1}\gamma_{1s} + \frac{I_{av,pv'} - I_{1s}}{2I_{1s}}\frac{\gamma_{1s}}{\sqrt{1+\gamma_{1s}^2}}, \tag{C3}$$

$$\eta_2 = -\frac{\gamma_{1s}}{\sqrt{1+\gamma_{1s}^2}} - \frac{I_{av,pv'} - I_{1s}}{2I_{1s}}\frac{\gamma_{1s}}{(1+\gamma_{1s}^2)^{3/2}}, \tag{C4}$$

$$\Xi_{j,j'}(\lambda+\lambda',\theta,\phi) = \int_0^\infty d\alpha\alpha^{\lambda+\lambda'+2}\exp\left\{-\left(\eta_1 + \eta_2\cos^2\theta + \frac{m\omega}{8\hbar\beta}\sin^2\theta\sin^2\phi\right)\alpha^2 + i\alpha\eta_3(j,j')\sin\theta\sin\varphi\right\}, \tag{C5}$$

$$\eta_3(j,j') = \frac{-(-1)^j + (-1)^{j'}}{2}\sqrt{\frac{m\omega}{\hbar}}\left(R_{0a} + \frac{\Delta R}{2}\right), \tag{C6}$$

and $j=1$ and $j'=2$, or $j=2$ and $j'=1$.

The integrations in Eqs. (C1), (C2), and (C5) have been performed numerically. For the integration over α in Eq. (C5), we have used the following formula:

$$\int_0^\infty d\alpha\exp(-A\alpha^2 + iB\alpha) = \frac{1}{2}\sqrt{\frac{\pi}{A}}\exp\left(-\frac{B^2}{4A}\right) + \frac{i}{\sqrt{A}}\exp\left(-\frac{B^2}{4A}\right)\int_0^{B/2\sqrt{A}}\exp(t^2)dt. \tag{C7}$$

From the above equations, we notice that the non-Condon approximation does not affect the exponential factor, but the preexponential factor is affected in the perpendicular polarization case.

We can see that the terms where $\lambda=0$ and $m\omega/8\hbar\beta=0$ on the rhs of Eq. (C1) for the individual photoionization rate, and $\lambda=\lambda'=0$ in Eq. (C2), $(m\omega/8\hbar\beta)\sin^2\theta\sin^2\phi=0$ in Eq. (C5), and $\Delta R/2=0$ in Eq. (C6) for the quantum interference terms correspond to those under the Condon approximation. The other terms stem purely from the non-Condon approximation. Comparing this with Eq. (2.46), we notice that under the non-Condon approximation, the parallel polarization case will be affected more than that of perpendicular case because the former contains many more terms.

As has already been shown above, the term $\Delta R/2$ in Eq. (C6) and the summations for $\lambda\neq 0$ or $\lambda'\neq 0$ purely stem from the non-Condon approximation. In their absence, Eq. (C2) reduces to Eq. (A6). $\Xi_{j,j'}(\lambda+\lambda',\theta,\phi)$ in Eq. (C5) can be calculated by using Eq. (C7). We can see that the nuclear distance R_{0a} does not affect the individual photoionization rates but the quantum interference terms are affected.

[1] L. V. Keldysh, Zh. Eksp. Teor. Fiz. **47**, 1945 (1964) [Sov. Phys. JETP **20**, 1307 (1965)].
[2] F. H. M. Faisal, J. Phys. B **6**, L89 (1973).
[3] H. R. Reiss, Phys. Rev. A **22**, 1786 (1980).
[4] M. V. Ammosov, N. B. Delone, and V. P. Krainov, Sov. Phys. JETP **64**, 1191 (1986).
[5] J. Muth-Böhm, A. Becker, and F. H. M. Faisal, Phys. Rev. Lett. **85**, 2280 (2000).
[6] X. M. Tong, Z. X. Zhao, and C. D. Lin, Phys. Rev. A **66**, 033402 (2002).
[7] A. Saenz, Phys. Rev. A **66**, 063408 (2002).
[8] A. Saenz, J. Phys. B **33**, 4365 (2000).
[9] T. D. G. Walsh, F. A. Ilkov, S. L. Chin, F. Chateauneuf, T. T. Nguyen-Dang, S. Chelkowski, A. D. Bandrauk, and O. Atabek, Phys. Rev. A **58**, 3922 (1998).
[10] A. Talebpour, C.-Y. Chien, and S. L. Chin, J. Phys. B **29**, L677 (1996).
[11] F. H. M. Faisal, A. Becker, and J. Muth-Böhm, Laser Phys. **9**, 115 (1999).
[12] S. Chelkowski, C. Foisy, and A. D. Bandrauk, Phys. Rev. A **57**, 1176 (1998); S. Chelkowski and A. D. Bandrauk, J. Phys. B **28**, L723 (1995); S. Chelkowski, T. Zuo, O. Atabek, and A. D. Bandrauk, *ibid.* **52**, 2977 (1995); H. Yu and A. D. Bandrauk, *ibid.* **56**, 685 (1997); I. Kawata, H. Kono, and A. D. Bandrauk, *ibid.* **64**, 043411 (2001); K. Harumiya, I. Kawata, H. Kono, and Y. Fujimura, J. Chem. Phys. **113**, 8953 (2000); I. Kawata, H. Kono, and Y. Fujimura, *ibid.* **110**, 11152 (1999); K. Harumiya, H. Kono, Y. Fujimura, I. Kawata, and A. D. Bandrauk, Phys. Rev. A **66**, 043403 (2002); I. Kawata, H. Kono, Y. Fujimura, and A. D. Bandrauk, *ibid.* **62**, 031401(R) (2000); I. Kawata, A. D. Bandrauk, H. Kono, and Y. Fujimura, Laser Phys. **11**, 181 (2001).
[13] K. Mishima, M. Hayashi, J. Yi, S. H. Lin, H. L. Selzle, and E. W. Schlag, Phys. Rev. A **66**, 033401 (2002); K. Mishima, M. Hayashi, J. Yi, S. H. Lin, H. L. Selzle, and E. W. Schlag, *ibid.* **66**, 053408 (2002).
[14] T. Zuo and A. D. Bandrauk, Phys. Rev. A **52**, R2511 (1995).
[15] F. H. M. Faisal and A. Becker, Laser Phys. **7**, 684 (1997).
[16] A. Becker and F. H. M. Faisal, Opt. Express **8**, 383 (2001).
[17] M. J. Frisch, G. W. Trucks, H. B. Schlegel, G. E. Scuseria, M. A. Robb, J. R. Cheeseman, V. G. Zakrzewski, J. A. Montgomery, Jr., R. E. Stratmann, J. C. Burant, S. Dapprich, J. M. Millam, A. D. Daniels, K. N. Kudin, M. C. Strain, O. Farkas, J. Tomasi, V. Barone, M. Cossi, R. Cammi, B. Mennucci, C. Pomelli, C. Adamo, S. Clifford, J. Ochterski, G. A. Petersson, P. Y. Ayala, Q. Cui, K. Morokuma, D. K. Malick, A. D. Rabuck, K. Raghavachari, J. B. Foresman, J. Cioslowski, J. V. Ortiz, B. B. Stefanov, G. Liu, A. Liashenko, P. Piskorz, I. Komaromi, R. Gomperts, R. L. Martin, D. J. Fox, T. Keith, M. A. Al-Laham, C. Y. Peng, A. Nanayakkara, C. Gonzalez, M. Challacombe, P. M. W. Gill, B. G. Johnson, W. Chen, M. W. Wong, J. L. Andres, M. Head-Gordon, E. S. Replogle, J. A. Pople, GAUSSIAN 98, revision A.11.2 (Gaussian, Inc., Pittsburgh, PA, 1998).
[18] F. V. Bunkin and I. I. Tugov, Phys. Rev. A **8**, 601 (1973).
[19] W. H. Press, B. P. Flannery, S. A. Teukolsky, and W. T. Vetterling, *Numerical Recipes in C* (Cambridge University Press, Cambridge, UK, 1988).
[20] M. S. Child, *Semiclassical Mechanics with Molecular Applications* (Clarendon, Oxford, 1991).
[21] A. Saenz, Phys. Rev. A **61**, 051402(R) (2000).
[22] A. Talebpour, S. Larochelle, and S. L. Chin, J. Phys. B **31**, L49 (1998).
[23] X. Urbain, B. Fabre, E. M. Staicu-Casagrande, N. de Ruette, V. M. Andrianarijaona, J. Jureta, J. H. Posthumus, A. Saenz, E. Baldit, and C. Cornaggia, Phys. Rev. Lett. **92**, 163004 (2004).